This chapter was originally published in the book *Progress in Brain Research, Vol. 228* published by Elsevier, and the attached copy is provided by Elsevier for the author's benefit and for the benefit of the author's institution, for non-commercial research and educational use including without limitation use in instruction at your institution, sending it to specific colleagues who know you, and providing a copy to your institution's administrator.

Neural and cortical analysis of swallowing and detection of motor imagery of swallow for dysphagia rehabilitation—A review

H. Yang*,[1], **K.K. Ang***,[†], **C. Wang***, **K.S. Phua***, **C. Guan***,[†]

*Neural and Biomedical Technology Department, Institute for Infocomm Research, A*STAR, Singapore
†School of Computer Science and Engineering, College of Engineering, Nanyang Technological University, Singapore
[1]Corresponding author: Tel.: +65-6408-2000; Fax: +65-6776-1378, e-mail address: hjyang@i2r.a-star.edu.sg

Abstract

Swallowing is an essential function in our daily life; nevertheless, stroke or other neurodegenerative diseases can cause the malfunction of swallowing function, ie, dysphagia. The objectives of this review are to understand the neural and cortical basis of swallowing and tongue, and review the latest techniques on the detection of motor imagery of swallow (MI-SW) and motor imagery of tongue movements (MI-TM), so that a practical system can be developed for the rehabilitation of poststroke dysphagia patients. Specifically, we firstly describe the swallowing process and how the swallowing function is assessed clinically. Secondly, we review the techniques that performed the neural and cortical analysis of swallowing and tongue based on different modalities such as functional magnetic resonance imaging, positron emission tomography, near-infrared spectroscopy (NIRS), and magnetoencephalography. Thirdly, we review the techniques that performed detection and analysis of MI-SW and MI-TM for dysphagia stroke rehabilitation based on electroencephalography (EEG) and NIRS. Finally, discussions on the advantages and limitations of the studies are presented; an example system and future research directions for the rehabilitation of stroke dysphagia patients are suggested.
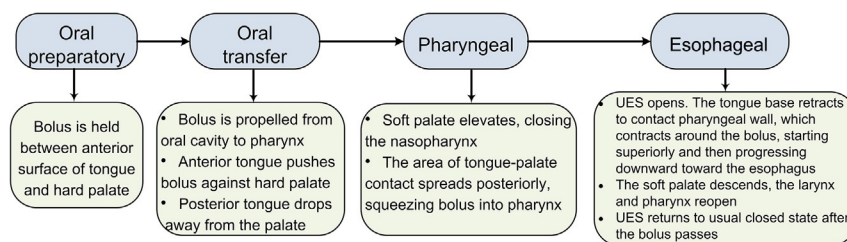
Keywords

1 BACKGROUND

1.1 INTRODUCTION

Human swallowing is a fundamental function that is essential to our daily life. Dysphagia is the difficulty in swallowing or the inability to swallow resulting from the injury to swallowing motor areas and their connection to the brain stem (Hamdy et al., 1999a,b, 2000, 2001). Dysphagia is usually caused by stroke or other neurodegenerative diseases and central nervous system disorders (Furlong et al., 2004; Jestrovic et al., 2015; Martin et al., 2004; Satow et al., 2004; Teismann et al., 2011; Yang et al., 2012, 2014). The initiation of swallowing is a voluntary action, which requires the integrity of sensorimotor areas of the cerebral cortex (Hamdy et al., 1999a,b), and a series of oral and pharyngesophageal peristaltic events (Furlong et al., 2004). Swallowing consists of a series of processes, namely, voluntary and reflex motor control, intraoral sensory processing, salivation, and visceral regulation (Satow et al., 2004). If any of these processes or connections to the brain stem were damaged, initiation of swallow would become difficult. The majority of dysphagia is caused by stroke, where most stroke patients experience dysphagia (Hamdy et al., 2000, 2001). Dysphagia can lead to series of consequences such as malnutrition, pulmonary aspiration, mortality, and poor quality of life.

Motor imagery is a mental process by which an individual rehearses or simulates a given action in his/her mind without actually performing the movement (Dickstein and Deutsch, 2007; Ge et al., 2014; Sharma et al., 2006). Brain–computer interfaces (BCIs) enable those patients who have lost control of their motor faculties to communicate with the external world through the imagination of actions such as movements of limbs and tongue (Morash et al., 2008; Wolpaw et al., 2002). Motor imagery is assumed to involve similar cortical brain areas as that activated during motor execution (Dickstein and Deutsch, 2007; Ge et al., 2014; Sharma et al., 2006), which has been employed to improve the sparsity and recovery of motor function for the rehabilitation of stroke patients (Ang et al., 2014a,b; Dickstein and Deutsch, 2007; Prasad et al., 2010; Sharma et al., 2006; Silvoni et al., 2011). Motivated by these works, several methods on the detection of motor imagery of swallow (MI-SW) have been proposed recently, with the aim of facilitating the motor imagery-based training of dysphagia stroke patients for rehabilitation (Yang et al., 2012, 2013a,b, 2014).

1.2 SWALLOWING PROCESS AND ASSESSMENT

Swallowing is a complex process that requires the sensory processing of ingested material; execution of oral, pharyngeal, and laryngeal movements; coordination with mastication and respiration (Martin et al., 2004). Swallowing consists of three interacting phases, ie, oral (oral preparatory and oral transfer), pharyngeal, and esophageal phases, which are of varying degrees of dependence on the central control mechanism (Ertekin and Aydogdu, 2003; Matsuo and Palmer, 2008; McKeown et al., 2002; Satow et al., 2004). Varying amount of functional and structural

| Oral preparatory | → | Oral transfer | → | Pharyngeal | → | Esophageal |

| Bolus is held between anterior surface of tongue and hard palate | • Bolus is propelled from oral cavity to pharynx
• Anterior tongue pushes bolus against hard palate
• Posterior tongue drops away from the palate | • Soft palate elevates, closing the nasopharynx
• The area of tongue-palate contact spreads posteriorly, squeezing bolus into pharynx | • UES opens. The tongue base retracts to contact pharyngeal wall, which contracts around the bolus, starting superiorly and then progressing downward toward the esophagus
• The soft palate descends, the larynx and pharynx reopen
• UES returns to usual closed state after the bolus passes |

FIG. 1

Block diagram of swallowing a liquid bolus.

Adapted from Matsuo, K., Palmer, J.B., 2008. Anatomy and physiology of feeding and swallowing: normal and abnormal. Phys. Med. Rehabil. Clin. N. Am. 19 (4), 691–707.

abnormality exist in dysphagia patients in each of these phases (Matsuo and Palmer, 2008; Mckeown et al., 2002), eg, oral cavity, pharynx, larynx, or esophagus. To initiate and regulate swallowing, combination of feedback and motor planning is required (Furlong et al., 2004). A block diagram of swallowing a liquid bolus is shown in Fig. 1.

Swallowing assessment is used to evaluate how safe a patient can swallow, which is usually done by a skilled speech–language pathologist (Mckeown et al., 2002). The assessment includes bedside assessment and video fluoroscopy. The bedside assessment assesses the feeding status, posture, breathing and cooperation levels, oral reflexes, pharyngeal swallow, and a trial feed with water bolus. Videofluoroscopy is an X-ray technique that provides a detailed anatomical assessment by illuminating the path taken by the bolus (mixed with barium) as it completes the four phases of swallowing (Hamdy et al., 2000; McKeown et al., 2002). The newer fiberoptic endoscopic evaluation of swallowing (FEES) technique enables more direct assessment (McKeown et al., 2002). FEES examines motor and sensory functions of swallowing so that proper treatment can be given to patients with swallowing difficulties. Conventional therapeutic interventions include the changes in diet, posture, and adjustments of food; the physical exercises such as tongue strengthening exercises and pharyngeal maneuvers; and methods for sensitizing/desensitizing the oropharynx to alter swallow reflex (Hamdy et al., 2000; Kiger et al., 2006). Recently, stimulation techniques such as thermal stimulation and neuromuscular stimulation (eg, VitalStim) were employed (Kiger et al., 2006; Langdon and Blacker, 2010).

1.3 OBJECTIVES AND MOTIVATION

The objectives of this review are on the following aspects. Firstly, we review and summarize the typical methodologies that performed the neural cortical analysis of swallowing and tongue protrusion and movements based on the modalities such as fMRI, PET, MEG, and NIRS. Secondly, we review the techniques that performed the detection of MI-SW, motor imagery of tongue protrusion/movements (MI-TM), and the analysis of the correlations between MI-SW and MI-TM, and between
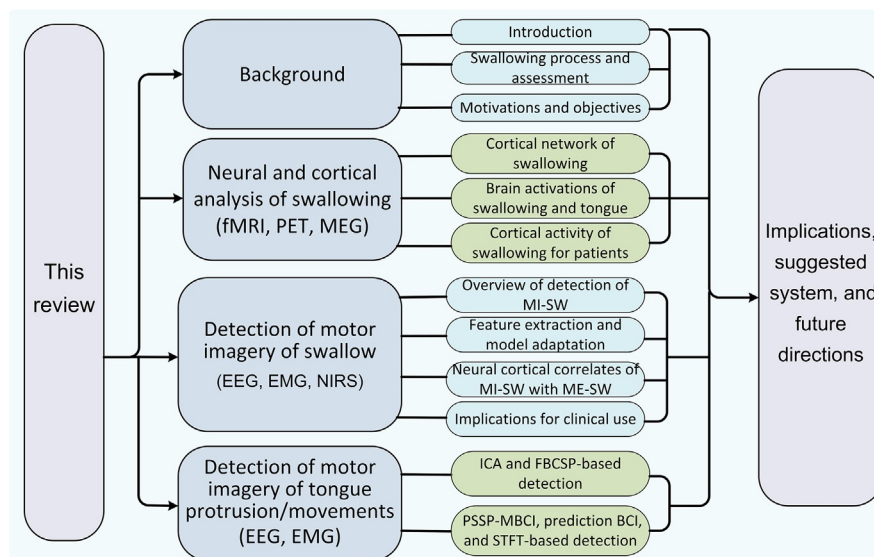
FIG. 2

Schematic illustration of the coverage in this review.

MI-SW and motor execution of swallow (ME-SW). Thirdly, we review existing work on the detection of MI-TM under multiclass settings. Finally, discussions on the advantages and limitations of the studies for swallowing are presented, and an example rehabilitation system and future research directions are suggested. The focus of this review is on BCI-based techniques, with the aim of proposing a motor imagery-based technique for the rehabilitation of stroke patients suffering from dysphagia. A schematic illustration of the coverage in this review is shown in Fig. 2. It is noted that the neurological origins of swallowing, cortical activations during swallowing, different modalities used for swallowing studies, and swallowing-related olfactory-based electroencephalography (EEG) studies have also been discussed in other reviews (Ertekin and Aydogdu, 2003; Jestrovic et al., 2015).

2 NEURAL AND CORTICAL ANALYSIS OF SWALLOWING

In this section, we review typical techniques used for neural and cortical analysis of the components of swallowing and summarize the details of the major articles in Table 1.

2.1 CORTICAL NETWORK OF SWALLOWING

The neuroanatomical representation of the cortical network involved in swallowing has been identified using transcranial magnetic stimulation (TMS) (Hamdy et al., 1996), functional magnetic imaging (Hamdy et al., 1999a,b), and positron emission

Table 1 Studies on Neural and Cortical Analysis of Swallowing

Category, Reference, Modality	Subjects and Cue, Data	Study Contents	Key Findings
Hamdy et al. (1996), TMS, Cortical network for swallowing	20 Healthy subj. (12/8: male/female, mean: 34); 2 stroke pat. (51 and 68, unilateral hemispheric stroke; 1 with/1 without dysphagia	To study cortical topography of human oral, pharyngeal, and esophageal musculature in healthy subj.; and topography of pharyngeal musculature in stroke pat. Apply single magnetoelectric stimuli to cortex to excite EMG responses. 3 stimuli for each scalp site	○ Swallowing musculature was represented by motor and premotor cortex, showed interhemispheric asymmetry, independent of handedness ○ Topography of the mylohyoid muscles was most lateral and that of pharynx and esophagus appeared to be more rostromedial ○ Dysphagia was associated with smaller pharyngeal representation on intact hemisphere and increased with the recovery of swallowing
Hamdy et al. (1999a), fMRI, Cortical network for swallowing	10 Healthy volunteers (7/3: male/female, mean age: 32 years); water bolus	To study cortical activations and lateralization Injecting water bolus into the oral cavity every 30 s	○ Areas with increased signal changes: caudal sensorimotor cortex, anterior insula, premotor cortex, frontal operculum, anterior cingulate and prefrontal cortex, anterolateral and posterior parietal cortex ○ Activations were bilateral, and lateralization was observed at premotor, insular, and frontal opercular cortices ○ Multidimensional cortical activity implied recruiting brain areas for processing motor, sensory, and attention/affective aspects of task
Martin et al. (2004), fMRI, Brain activations for swallowing and tongue	14 Healthy subj. (12/2: female/male, 28±6.5 years), performed voluntary saliva swallowing, tongue mov., finger opposition Visual cues	Single-event-related fMRI, laryngeal, and tongue movements were recorded 12-min imaging runs, 3 tasks in each run: voluntary swallowing of saliva, voluntary tongue elevation, and finger opposition, 6 times for each task	○ Both swallowing and tongue elevation activated left lateral pericentral and anterior parietal cortex; anterior cingulate cortex and adjacent SMA. Tongue activation was larger than swallowing at ACC, SMA, right precentral and postcentral gyri, premotor cortex, right putamen, and thalamus ○ 60% of the subjects showed lateralization of the postcentral gyrus toward left hemisphere for swallowing. 40% showed lateralization toward left for tongue elevation

Table 1 Studies on Neural and Cortical Analysis of Swallowing—cont'd

Category, Reference, Modality	Subjects and Cue, Data	Study Contents	Key Findings
Furlong et al. (2004), MEG, Brain activations for swallowing and tongue	8 Healthy subj. (6/2: male/female, aged 28–45), 151-channel whole cortex MEG data were collected	To study temporal characteristics of cortical activity of swallowing using MEG. Oral water infusion, volitional wet swallowing (5 mL bolus), tongue thrust, or rest. Each condition lasted for 5 s and was repeated 20 times. SAM analysis was performed	○ Water infusion preferentially activated caudolateral sensorimotor cortex. Volitional swallowing and tongue movement activated superior sensorimotor cortex ○ Time–frequency wavelet analysis showed that sensory input from tongue simultaneously activated caudolateral sensorimotor and primary gustatory cortex (prime areas for volitional phase of swallowing)
Satow et al. (2004), scalp EEG and epicortical EEG Brain activations for swallowing and tongue	8 Healthy subj. (7/1: male/female, 24–38), scalp EEG. 6 epilepsy pat. (2/4: male/female, 15–34), implanted Subdural elec., self-paced, each sess. 10 min, 8–10 sess.	To investigate face/tongue SMI and SMA in volitional swallowing by MRCPs. To determine hemispheric dominance from preparatory phase of swallowing (scalp EEG). Swallow: keep 2–3 mL water in mouth and swallow with jaw kept relaxed and slightly open. Tongue: jaw was kept relaxed, to make brisk forward protrusion of tongue	○ Scalp EEG for normal subjects revealed that premovement BP was largest at vertex and lateralized ○ Epicortical EEG in patients confirmed that face/tongue SMI and SMA were involved in swallowing and tongue protrusion. SMA played a supplementary role to face/tongue SMI in swallowing and tongue ○ No difference in BP amplitude between swallowing and tongue, whereas PMP was significantly larger in tongue than swallowing at face/tongue SMI, suggesting cerebral cortex does not play a significant role in postmovement processing of swallowing
Teismann et al. (2011) Cortical activity of swallowing for patients	7 Controls (3/4: female/male, mean: 57.6), 14 ALS (9/5: male/female, mean: 58.9), mildly (MDG, 7) and severely dysphagic (SDG, 7) patients	Investigated cortical activation during deglutition in MDG and SDG ALS using MEG Performed time–frequency analysis and SAM. 15 min of MEG recording, swallowed in self-paced manner, no external cue. Data were collected by 275-channel SQUID array	○ Reduction in cortical swallowing-related activation in ALS, the response was stronger for SDG group ○ Healthy subjects showed bilateral cortical activation, whereas the right sensorimotor cortex was dominant for ALS patients ○ The cortical plasticity demonstrated by the right hemisphere lateralization (RHL) of volitional swallowing can be used as compensational mechanisms, where the RHL is known to predominantly coordinate the pharyngeal phase of deglutition

Notes: subj., *subjects;* pat., *patients;* mov., *movements;* sess., *session;* elec., *electrodes;* ALS, *amyotrophic lateral sclerosis;* ACC, *anterior cingulate cortex;* SMA, *supplementary motor area;* BP, *Bereischaftspotentials;* PMP, *postmovement potential;* MDG, *mildly dysphagic patients;* SDG, *severely dysphagic patients;* SMI, *face/tongue area of primary sensorimotor.*

tomography (PET) (Hamdy et al., 1999a,b). A review of the swallowing problems and how the organization of the cortical projections to swallowing muscles can account for many clinical observations on swallowing after stroke has been reported (Hamdy et al., 2000, 2001). The central nervous system of the brain controls the regulation of swallowing (Hamdy et al., 2000). Specifically, the reflective component of swallowing depends on the swallowing center in the brain stem, whereas the initiation of swallowing is voluntary involving the integrity of motor areas of cerebral cortex (Hamdy et al., 2000). Furthermore studies showed that one of the hemispheres was dominant on the control of swallowing for humans (Hamdy et al., 2000). Asymmetry was found in the size of responses evoked by a constant stimulus to each hemisphere (Hamdy et al., 1997a, 1998, 2000, 2001), ie, the responses from one hemisphere tended to be larger than that of another. Analysis of the electromyogram (EMG) response from stimulation of a single shocks given several seconds apart showed that the EMG had a latency comparable to the pathway from the cortex via brain stem to the muscles (Hamdy et al., 2000), demonstrating the somatotopically arranged swallowing muscles such as the oral muscles, and the pharynx and esophagus were arranged laterally and medially, respectively. The PET results on swallowing showed strong activations in the sensorimotor cortices, insula, and cerebellum (Hamdy et al., 2000). Other cerebral regions that were recruited in an asymmetric manner are right orbitofrontal cortex, left medial premotor cortex and cingulate, right and left caudolateral sensorimotor cortex, right anterior insular, left temporopolar cortex merging with left amygdala, right temporopolar cortex, and left medial cerebellum.

The physiological characteristics of the corticofugal pathways to oral, pharyngeal, and esophageal muscles help identify their topographic relations and explore the evidence for interhemispheric asymmetries described (Hamdy et al., 1996). TMS was given by single magnetoelectric stimuli to the cortex of fully conscious subjects, which evoked the EMG responses in each of the individual muscle groups active in the swallowing. The evoked EMG responses show that the individual muscle groups respond bilaterally and are asymmetrically represented in the motor and premotor cortex (Hamdy et al., 1996). This finding inferred an important role of the motor cortex in the control of the complex swallowing process. It is anticipated that the specific areas of the motor cortex may be related to each phase of swallowing, which may act differently from the brain stem swallowing center and can be modulated individually to control and monitor the swallowing process.

To understand how the cerebral cortex operates in controlling the complex swallowing function, the cortical activity associated with human volitional swallowing using single-event-related functional magnetic resonance imaging (fMRI) was identified (Hamdy et al., 1999a). The water boluses of 5 mL were injected into the oral cavity every 30 s via a plastic infusion catheter, and the subject was instructed to initiate swallowing. Each subject performed 20 wet swallows. The analysis results showed that the peak activation occurred at least 12 s after onset of swallow. Most subjects showed a significant decrease in signal change immediately after swallow. Consistent activations are observed in ACC, caudolateral sensorimotor cortex,

anterior insula, frontal opercular cortex, superior premotor cortex, anteromedial temporal cortex, anterolateral somatosensory cortex, and precuneus (Hamdy et al., 1999a). Activations were bilateral for most subjects; however, they were lateralized at insular, opercular, and premotor cortices, which was consistent with the results reported in Hamdy et al. (1996, 1999b), showing that the motor projections of pharyngeal and esophageal from areas anterior to the primary motor strip are asymmetrically represented (Hamdy et al., 1999a,b). These results furthermore imply that the cortical control mechanisms are more important for pharyngeal and esophageal motility than oral stage functions.

Compensatory reorganization of the undamaged hemisphere has been suggested for the recovery of swallowing function in the throat (Hamdy et al., 2000). One possible therapy to speed up the recovery is to manipulate the sensory input to the cortex. Another way is to induce changes in the excitation of motor cortex with prolonged electrical stimulation of the pharynx for up to 15 min (Hamdy et al., 1998, 2000). These findings can be exploited for the treatment of the dysphagia patients by noting the asymmetry on the connections of each hemisphere, increasing the involvement of the projections from the undamaged hemisphere, and involving the stimulation of sensory and afferent inputs from the pharynx (Hamdy et al., 2000, 2001). The pharyngeal responses to swallowing show a remarkable increase in amplitude and area for unaffected hemisphere, compared with the little changes showed in the affected hemisphere (Hamdy et al., 2000).

The key points of these findings are summarized in the reviews (Hamdy et al., 2000, 2001). Cerebral cortex plays an important role in regulation of swallowing and the reflexive component of swallowing depends on swallowing centers in brain stem. Initiation of swallowing involves the integrity of motor areas of cerebral cortex. The locus of cortical control of swallowing lies anterior caudal to the face area of primary motor cortex. The most effective site for stimulation is slightly anterior to the best points for obtaining responses in muscles of hand or arm. Repetitive electrical stimulation of cortex in animals or humans can help induce swallowing (Hamdy et al., 2001). One of the hemispheres is dominant, whereas stimulation of undamaged hemisphere of dysphagia patients produces smaller responses in pharynx and esophagus than that of the undamaged hemisphere in nondysphagic patients. This finding can be used to determine the presence or absence of dysphagia. Good recovery of swallowing function depends on compensatory reorganization of the undamaged hemisphere. Future therapies could target at interventions for reorganization on the intact side to enhance swallowing.

2.2 BRAIN ACTIVATIONS OF SWALLOWING AND TONGUE

Swallowing and tongue are relevant but distinct actions, whereas tongue movement is an integral part of swallowing process. Hence, investigations have been carried out to study the brain activations during swallowing and tongue movements based on fMRI (Martin et al., 2004), magnetoencephalography (MEG) (Furlong et al., 2004) and movement-related cortical potentials (MRCPs) (Satow et al., 2004). Trials

of single swallowing and tongue elevation were verified based on profiles of laryngeal movements (Martin et al., 2001, 2004). The brain activations for swallowing and tongue elevation were contrasted and identified (Martin et al., 2004). The inclusion of tongue elevation lies in that it is an integral part of swallowing and can be produced volitionally. The inclusion of finger opposition task is to verify that the brain regions activated by swallow or tongue elevation is specific to an oral sensorimotor task, and not to the limb movements. The common activated regions of swallowing and tongue elevation were interpreted as the motor planning and motor execution shared by them. The brain regions activated by swallowing but not tongue elevation were interpreted as the functional role performed specific to swallowing regulation (Martin et al., 2002, 2004). The results showed that the most consistent shared common activation regions were the lateral pericentral cortex, frontoparietal operculum, and ACC. The pericentral activation common to both tasks may show the mechanical sensory stimulation of the oral cavity by moving the bolus during swallow, as well as by the tongue contacting with other oral tissues (Martin et al., 2004). The distinct activation regions of swallowing and tongue movements from that of finger tapping were consistent with previous findings that the orofacial representation within sensorimotor cortex was lateral to that the hand (Mosier et al., 1999). The common activated frontoparietal operculum suggests that the presence of the mediation of the similar processing during simple voluntary oral movements such as tongue elevation (Martin et al., 2001). Furthermore, the common activated region of somatosensory association areas may also suggest that the mechanical sensory processing (rather than gustatory processing) is involved in tongue elevation since tongue movement does not involve the manipulation of the bolus (Martin et al., 2004). The regions activated by swallowing alone were left lateral pericentral cortex immediately lateral to the area activated by tongue movement, left postcentral gyrus, ACC, precuneus/cuneus, and right insula/operculum (Martin et al., 2004).

A synthetic aperture magnetometry (SAM)-based technique for MEG data was employed to dissociate the cortical contributions of each separable component of swallowing in the sensorimotor sequence and identify the spatiotemporal characteristics of cortical activity during swallowing (Furlong et al., 2004). The MEG data were analyzed in the frequency bands of 5–15 Hz, 15–25 Hz, and 25–40 Hz. The active epochs windowed at 5 s following the cues to receive water, swallow, or tongue thrust were referenced to the passive epochs of 5 s before cue to rest. The event-related paradigm makes it possible to separate the components of swallowing. Time–frequency plots based on wavelet analysis were employed to examine the temporal sequencing of activation within regions of interest (ROIs). SAM was then used to dissociate both the spatial and temporal characteristics of cortical activity within an interconnected cortical swallowing network (Furlong et al., 2004).

Comparison of time–frequency wavelet plots for all subjects from left caudolateral precentral gyrus (dot in the image) before nonparametric statistical analysis is shown in Fig. 3. In the figure, the MRI-SAM group mean images for all eight subjects were shown in the right, where each active phase vs rest phase for the 15–25 Hz bands is shown. Significant activation within the left and right superior precentral
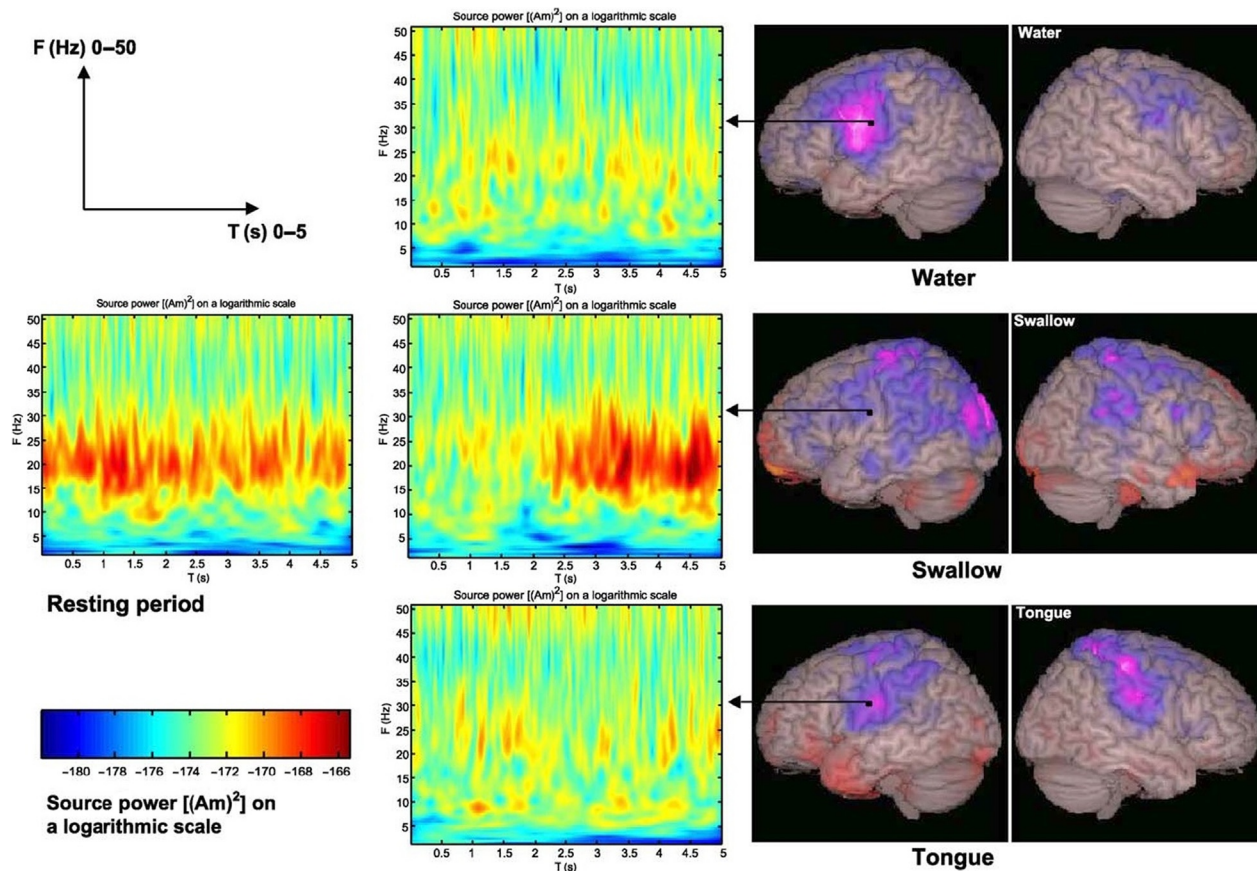
FIG. 3

Comparison of time–frequency plots for all subjects from left caudolateral precentral gyrus. Colors represented the level of frequency power difference between active and passive phases, with *blues* (*dark gray* in the print version)/*purples* (*gray* in the print version), and *reds* (*gray* in the print version)/*yellows* (*light gray* in the print version) indicating a decrease (ERD) and an increase (ERS) in power, respectively. Time 0 on the *x*-axis corresponds to the onset of the visual cue for each condition.

Reprinted from Furlong, P.L., Hobson, A.R., Aziz, Q., Barnes, G.R., Singh, K.D., Hillebrand, A., Thompson, D.G., and Hamdy, S., 2004. Dissociating the spatiotemporal characteristics of cortical neuronal activity associated with human volitional swallowing in the healthy adult. Neuroimage 22, 1447–1455, with permission from Elsevier.

gyrus (BA 4) together with the right postcentral gyrus in the 5–15 Hz frequency band and a larger area of activation in the inferior precentral cortex which appeared bilaterally was observed. The time–frequency wavelet plot for multiple cortical sites for one representative individual is shown in Fig. 4. Significant changes in power ($p < 0.05$) with respect to the mean level in the passive phase are indicated. The pattern of activation over time at an inferior precentral gyrus site was revealed. The selection of this site was due to the involvement of the precentral in all three active phases across all subjects. A dominant resting frequency in 15–25 Hz band was observed. The group SAM images showed the event-related desynchronization (ERD) throughout the water infusion and tongue thrust phases and the ERD during swallowing phase but with an event-related synchronization (ERS) rebound upon completion of swallowing.

The results showed that activation of superior sensorimotor cortex occurred during volitional swallowing and tongue movement, and caudolateral sensorimotor cortex was activated during water infusion. The ERD/ERS associated with swallowing was similar to those described by other functional imaging techniques. The findings with oral infusion of water confirmed that the sensation played a major role in central regulatory feedback of swallowing, acting at both brain stem and cortical levels (Furlong et al., 2004). The results revealed that the superior regions of precentral cortex were an important contributor to swallowing. The pericentral cortical loci activated during tongue movements was the same as that activated by swallowing, demonstrating that the significant contribution of tongue during swallowing was sensory. The temporal analysis of ROIs showed significant ERD following water infusion at the caudolateral pericentral cortex.

MRCPs preceding voluntary movements are known to reflect a central control process with superior temporal resolution (Satow et al., 2004). To clearly distinguish the motor components and sensory feedback, MRCPs at face/tongue area of primary sensorimotor (SMI) cortex and supplementary motor area (SMA) were employed to clarify the sequential cerebral processing of swallowing (Satow et al., 2004), where scalp EEG was recorded for normal subjects and epicortical EEG was recorded for patients. The changes of cortical activity in different phases of swallowing were also studied by MRCPs (Satow et al., 2004). As indicated, the pre- and postmovement activities of MRCPs reflected motor components without and with sensory feedback. Electrooculograms, EMG, and glossokinetic potential were recorded to monitor the eye movements and other swallow-related movements. Artifactual and incomplete trials were excluded, and the EEG signal was baseline corrected. The Bereitschaftspotentials (BP) onset time was determined visually at the time when slow potential shift started to arise from baseline (Satow et al., 2004). Two electrodes at the left (C3) and right (C4) central were used to determine the dominant side. The results revealed that the BP was maximal at the midline vertex for both swallow and tongue, and asymmetrically distributed, but the dominant side was not consistent across subjects, with the distribution of tongue to a lesser degree. The face/tongue SMI or its adjacent area was involved in BP generation for tongue but not for swallow. The amplitude of postmovement potential (PMP) on lateral for tongue was
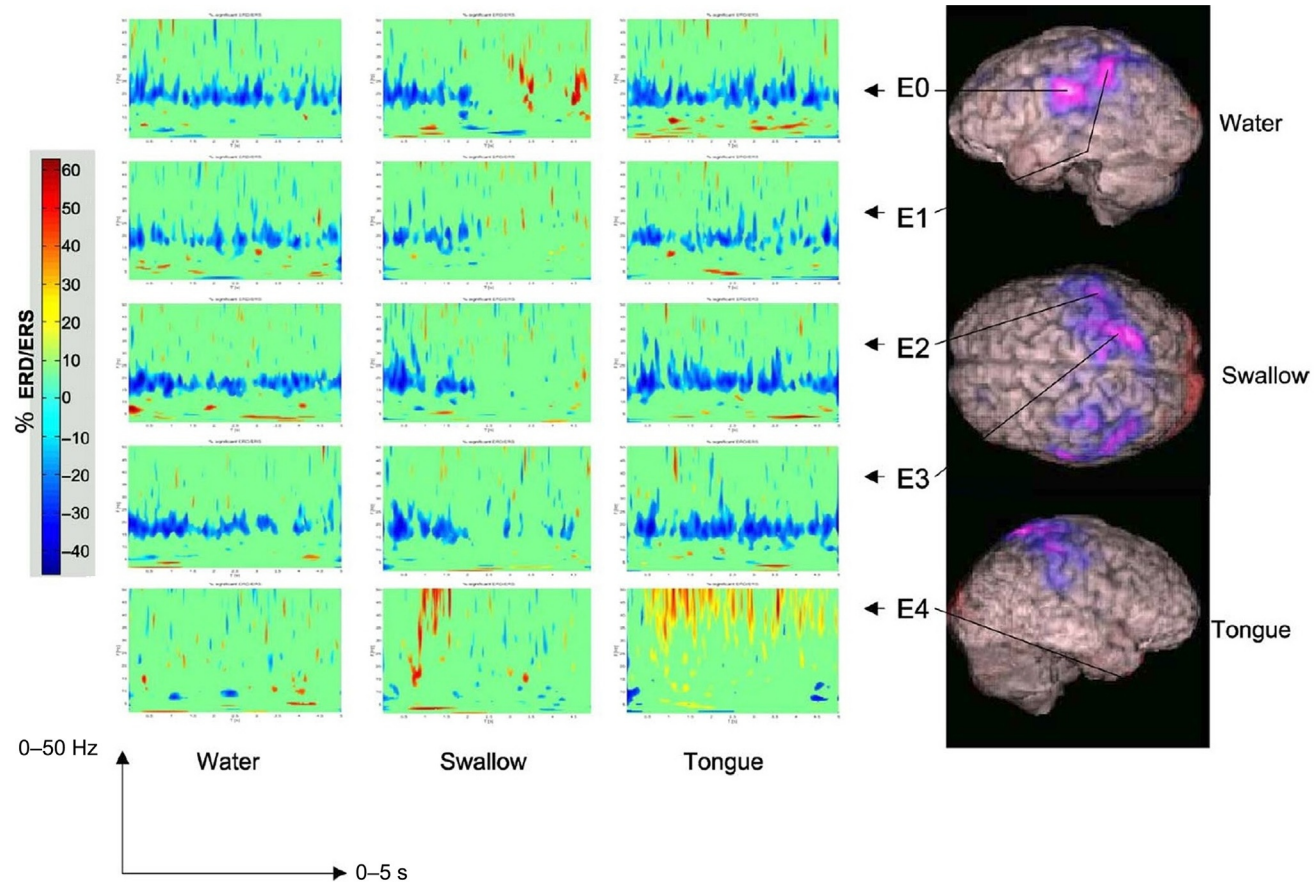
FIG. 4

Time–frequency wavelet plots for multiple cortical sites in one representative individual. Spectrograms calculated for a single subject. Voxels in positions E0, E1, E2, E3 represented the precentral gyrus, inferior parietal lobule, postcentral gyrus (Brodmann area 2), and postcentral gyrus (Brodmann area 5), respectively. MRI-SAM images (right) for the active water (25–40 Hz), swallow, and tongue thrust (15–25 Hz) phases vs rest. Time 0 on the x-axis indicates the end of the 5 s of the passive period and 0 s for the commencement of the 5 s of the active phase.

Reprinted from Furlong, P.L., Hobson, A.R., Aziz, Q., Barnes, G.R., Singh, K.D., Hillebrand, A., Thompson, D.G., and Hamdy, S., 2004. Dissociating the spatiotemporal characteristics of cortical neuronal activity associated with human volitional swallowing in the healthy adult. Neuroimage 22, 1447–1455, with permission from Elsevier.

significantly larger than that for swallow, despite the fact that swallowing is comprised of a sequence of motor and sensory processing. This suggests that the brain stem reflex mechanism is the main driving force for swallowing after initial volitional swallowing (Satow et al., 2004). Caudal SMA and rostral SMA were active in both swallow and tongue. No consistent difference on the distribution of BP and PMP between swallow and tongue on lateral or medial was found. The active areas for swallow and tongue overlapped to certain degrees, which may suggest that the face/tongue SMI played an equally important role in both the preparation for voluntary swallowing and tongue protrusion at least for the initial stage (Satow et al., 2004). The onset time of BP for swallow is earlier than that for tongue. The results furthermore demonstrated the engagement of face/tongue SMI in the preparation for volitional swallowing as well as tongue movement. Medial frontal cortex (caudal/rostral SMA) was commonly involved in volitional swallowing and tongue movements (Satow et al., 2004).

2.3 CORTICAL ACTIVITY OF SWALLOWING FOR PATIENTS

MEG has been employed to monitor the cortical activity with a high temporal and spatial resolution. The SAM-based whole-head MEG has been demonstrated as a reliable method to examine complex function of swallowing in humans (Furlong et al., 2004; Teismann et al., 2011). Along the same line, a whole-head MEG and SAM were employed to study the cortical activity during self-paced volitional swallowing for the amyotrophic lateral sclerosis (ALS) patients, aiming at discovering the effects of neuron degeneration of ALS to the cortical processing of human swallowing (Teismann et al., 2011). MEG data recorded from three groups of subjects, ie, control, mildly dysphagic patients (MDG), and severely dysphagic patients (SDG) were analyzed. The individual SAM results showed that ERD of beta and low gamma frequency band was bilateral in the sensorimotor cortices during swallowing execution phase for the controls. Left hemispheric lateralization was also observed for beta activation in the controls. Beta ERD was found in MDG and SDG patients, and most of them showed right hemispheric lateralization. No symmetric activation was found in all three groups. Group comparisons revealed significantly stronger activation of bilateral primary sensorimotor cortex in the control group compared with the patient groups. The significant reduction in cortical sensorimotor activation in ALS compared with controls increased with the progression of the disease. Furthermore, clear right hemispheric lateralization was observed in both patient groups (Teismann et al., 2011). The lack of involvement of the mesial areas or the secondary sensorimotor cortex but only the central area of the primary motor cortex might reflect the disturbance of the swallowing network (Teismann et al., 2011). Reasons for the reduction of the bilateral cortical ERD during swallowing may be due to the degeneration of the upper motor function or the compensation for the disordered pharyngeal swallowing by an increase in the number of active neurons at the right hemisphere (Teismann et al., 2011).

3 DETECTION OF MI-SW

In this section, we review different approaches on the detection and analysis of MI-SW and MI-TM based on EEG and near-infrared spectroscopy (NIRS). The details of these methods are summarized in Table 2.

3.1 OVERVIEW OF DETECTION OF MI-SW

Detection of MI-SW in comparison with the detection of MI-TM for the purpose of stroke dysphagia rehabilitation was investigated (Yang et al., 2012, 2013a,b, 2014, 2015a). BCI-based motor imagery of upper limb (eg, grasping, stretching, finger-typing, finger opposition, supination, pronation, etc.) and motor imagery of lower limb (eg, walking and foot dorsiflexion.) have been employed for stroke rehabilitation (Ang and Guan, 2015; Ang et al., 2014a,b; de Vries and Mulder, 2007; Dickstein et al., 2004; Do et al., 2011, 2013; Dunsky et al., 2008; Prasad et al., 2010; Sharma et al., 2006; Silvoni et al., 2011; Yang et al., 2015b). The principle is based on the shared common brain activation areas for motor imagery and motor execution of the same actions, eg, hand grasping and walking. The clinical trials based on 21 chronic hemiplegic stroke patients in BCI-haptic knob intervention, and the one based on 26 stroke patients in BCI-Manus therapy achieved significant higher motor gain compared with standard arm therapy, supporting its potential use in stroke rehabilitation coupled with physical rehabilitation therapy (Ang et al., 2014a,b). The engagement of the patients was measured during an MI practice by the neurofeedback, which was performed as part of the poststroke rehabilitation protocol, in conjunction with the physical practice (Prasad et al., 2010). Hemispheric asymmetry in both mu and beta bands contributed to BCI classification accuracies as demonstrated by the high correlation between classification accuracies and ERD/ERS ratios. Employing MI of upper limb or lower limb for the training of stroke patients has been investigated extensively in the past decades. However, there are only a few approaches that detected MI-SW for the rehabilitation of stroke dysphagia patients (Yang et al., 2012, 2013a,b, 2014). Possible reasons are as follows. First, swallowing is a complex process which involves the three phases of oral, pharyngeal, and esophageal and requires the integration from central nervous system, motor planning and control, attention, etc. It is difficult to imagine such a complex process especially for the dysphagia patients (Ertekin and Aydogdu, 2003; Yang et al., 2012, 2014). Second, detection of MI-SW is also difficult compared with that of motor imagery of upper limb and lower limb, where a single or only a few motor actions are involved.

The use of MI-SW for dysphagia rehabilitation was first investigated (Yang et al., 2012, 2013a,b, 2014, 2015a,b). In these studies, they investigated the following: (1) to test the hypotheses that MI-SW and MI-TM could be detected from the background idle state for their possible use in stroke dysphagia rehabilitation, (2) to build a model based on a simple yet relevant modality of MI-TM EEG signals to detect MI-SW, (3) to test the hypotheses by determining the classification accuracies across

Table 2 Studies on the Detection and Analysis of Motor Imagery of Swallow

Study	# of Subjects, Trials, Classes, and Cue	Modalities/ Electrodes	Features, Classifiers	Accuracies/Statistical Analysis Results and Key Findings
Yang et al. (2012)	6 Healthy subj. Cue: images; 60 trials/sess., 2 classes. MI-SW vs idle: 2 sess.; ME-TM vs idle: 1 sess.	EEG (MI-SW, ME-TM, Idle), 30 channels	Features: DTCWT; classifier: SVM	CV acc.: 69.96% Selecting the time segments based on the initiation from EEG signal of tongue movements is effective
Yang et al. (2013a)	6 Healthy subj. whose CV acc. >60%. Cue: Videos; 160 trials/sess. 2 sess., 2 classes: MI-SW vs idle	EEG (MI-SW, idle), 30 channels	Features: DTCWT; Laplacian power; classifier: SVM	○ S2S acc. using MI-SW model: 74.29% (power fea.) 72.64% (wavelet fea.) ○ Feature consistency and cluster impurity-based model adaptation (MA-FCCI) was effective for session-to-session classification based on MI-SW model
Yang et al. (2013b)	6 Healthy subj., CV acc. >60%. Cue: videos; 160 trials/sess., 2 classes. MI-SW vs idle: 2 sess.; MI-TM vs idle: 1 sess.	EEG, (MI-SW vs idle; MI-TM vs idle), 30 channels	Features: DTCWT; classifier: SVM	○ S2S acc.: 72.12% (using MI-SW model.) and 71.81% (using MI-TM model) ○ Using MI-TM model to classify MI-SW and model adaption using MA-FCCI was effective for session-to-session classification
Yang et al. (2014)	10 Healthy subj., 1 stroke patient. Cue: videos; 160 trials/sess., 2 classes. MI-SW vs idle: 2 sess.; MI-TM vs idle: 1 sess.	EEG (MI-SW vs idle; MI-TM vs idle), 30 channels	Features: DTCWT; classifier: SVM	○ CV acc.: 70.89% (MI-SW); 73.79% (MI-TM); S2S acc.: 66.40% (using MI-SW model); 70.24% (using MI-TM model) ○ MI-SW and MI-TM were detectable for healthy and dysphagia patient, using MI-TM and MI-SW model. Model adaptation by maximizing the ratio of the between-classes distance and within-class distances (MA-RBWD) was effective

Table 2 Studies on the Detection and Analysis of Motor Imagery of Swallow—cont'd

Study	# of Subjects, Trials, Classes, and Cue	Modalities/ Electrodes	Features, Classifiers	Accuracies/Statistical Analysis Results and Key Findings
Yang et al. (2015a,b)	10 Healthy subj., 1 stroke patient; cue: videos; 80 trials/ class, 3 classes: MI-SW, ME-SW, MI-TM	EEG (MI-SW, MI-TM, ME-SW), selected channels (C3, C4)	Bin-based spectral power, baseline removed, smoothed, spike trials corrected	○ Group analysis results demonstrated that MI-SW and MI-TM, and MI-SW and ME-SW were strongly correlated (p-value < 0.001, examined at "C3") for both mu and low beta frequency bands ○ Correlation was weaker but still significant for MI-SW and ME-SW (p-value < 0.05), and MI-SW and MI-TM (p-value < 0.01) for the dysphagia patient
Kober and Wood (2014)	14 Healthy subj. Cue: text; 20 trials/MI-SW and 20 trials/ ME-SW (swallow water)	NIRS (oxy-Hb, deoxy-Hb), 48 channels	PASW statistics 18 was used for statistical analysis	○ MI and ME showed strongest changes in inferior frontal gyrus. Changes in deoxy-Hb were comparable between kinesthetic MI and ME ○ ME: oxy-Hb significantly increased, peak at 15 s after task onset. MI: oxy-Hb decreased during MI compared to a rest period
Kober et al. (2015)	Patients: 2 with cerebral lesions, 2 with lesions in brain stem; 2 healthy subj.; Cue: text; 10 trials/MI-SW, 10 trials/ ME-SW, 2 classes, swallow saliva	NIRS (oxy-Hb, deoxy-Hb), 20 channels	Artifacts correction, high-pass and low-pass filtering, baseline correction, averaging task period	○ Patients with lesions in brain stem showed bilateral hemodynamic changes in inferior frontal gyrus during ME-SW ○ Patients with cerebral lesion showed more unilateral activation patterns during ME-SW and showed a prolonged time course during MI-SW and ME-SW compared to controls ○ Patients with brain stem lesions, activation patterns were largely comparable, especially for changes in deoxy-Hb (ME-SW and MI-SW)

Notes*: S2S, session-to-session; CV, crossvalidation; DTCWT, dual-tree complex wavelet transform; SVM, support vector machine; oxy-Hb, oxyhemoglobin; deoxy-Hb, deoxygenated hemoglobin; PASW, predictive analytics software.*

sessions and modalities, and (4) to determine the classification accuracies in a sample of 10 healthy volunteers and 1 subject with chronic stroke. Dual-tree complex wavelet transform (DTCWT) was employed for feature extraction (FE), in particular, the energy and phases of the wavelet coefficients at different levels and directions, and coarse representation of the EEG signal were used as the features. These signals are expected to contain the EEG rhythms at different frequency ranges, ie, the ERS and ERD. The dynamic initiation location identified using the EMG signal of tongue movements was employed to extract the effective time segment for the detection of MI-SW. This is possible since swallowing and tongue movements shared some common brain activation areas (Martin et al., 2004; Yang et al., 2014), whereby the tongue movements are an integral part of the whole swallowing process (Yang et al., 2012, 2014). Furthermore, the initiations to the motor imagery of two relevant tasks are expected to be similar for a person. Based on the selected six healthy subjects, an average classification accuracy (ie, by classifying MI-SW vs idle) of 69.96% was achieved by using the time segment centered at the dynamically identified initiation location of tongue movements. This was significantly higher than that obtained by using a fixed time segment with different time intervals, as well as the three existing methods, namely, common spatial pattern (CSP), filter bank CSP (FBCSP), and sliding window discriminative CSP (SWDCSP)-based methods. It should be noted that the timing for performing MI-SW was only 6 s in this experimental protocol, which is relatively short for a subject to complete the whole complex MI-SW process. The results also showed that choosing different sizes of moving window to detect the dynamic initiation time did not affect the detection rate significantly.

Furthermore investigations on how to improve the detection accuracies of classifying MI-SW vs idle based on MI-SW model (ie, the training model generated by classifying MI-SW vs idle) as well as MI-TM model (ie, the training model generated by classifying MI-TM vs idle) from earlier sessions were investigated (Yang et al., 2013a,b, 2014). The nonstationarity of EEG signal leads to the degradation of the classification performance, especially when the model was built using the data collected in a session which was far from the testing session. Two novel methods for model adaptation for the detection of MI-SW was proposed (Yang et al., 2013a,b, 2014), namely, model adaption based on the feature consistency and cluster impurity (MA-FCCI) (Yang et al., 2013a,b) and model adaptation by maximizing the ratio of between-classes distance and within-class distance (MA-RBWD) (Yang et al., 2014). A small amount of calibration-testing data collected on the same day as the testing data were employed to select the best training models to classify the testing data. The model adaptation methods were tested for classifying MI-SW vs idle using both MI-SW model and MI-TM model. These two methods will be discussed in more details in Section 3.2.2.

Moving the research from laboratory to clinical trials, in another attempt, detection of MI-SW and MI-TM was investigated based on 10 healthy subjects and 1 dysphagia patient (Yang et al., 2014). The session-to-session classification accuracy was boosted by adaptively selecting the trained models. In this investigation,
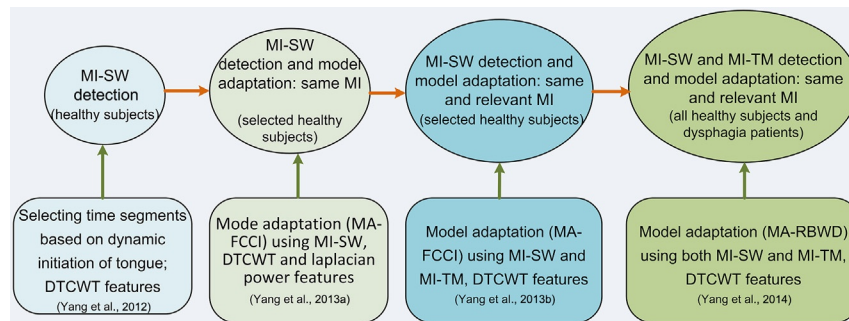
FIG. 5

Schematic illustration of the progression of DTCWT-based detection of MI-SW and MI-TM.

10 healthy subjects with the mean age of 35.9 ± 7.7 years old (mean $\pm$ standard deviation), and one stroke dysphagia patient of 56-year-old Chinese male participated in the experiments (Yang et al., 2014). The experimental protocol consisted of 17 s including 2 s of preparation and 15 s of performing MI-SW or MI-TM (tongue protrusion). This long time interval allowed the subject to finish the imagination of the complex swallowing process. Two sessions of MI-SW and one session of MI-TM EEG data were collected. These data were used to test the session-to-session classification accuracy using the proposed adaptive model selection method and to test the possibility of using MI-TM model to classify MI-SW. In these experiments, Neuroscan NuAmps cap and EEG acquisition software were employed. EMG activity was also monitored by recording the activities at the submental and infrahyoid muscles. A schematic illustration of the progression of the detection of MI-SW and MI-TM for dysphagia rehabilitation based on EEG signals is shown in Fig. 5.

3.2 FEATURE EXTRACTION AND MODEL ADAPTATION
3.2.1 Feature extraction
CSP has been widely employed in extracting features for EEG signals (Blankertz et al., 2008; Ramoser et al., 2000). CSP transforms the data into the two classes such that they have the same principle components, and their eigen values added up to a unit matrix (Ge et al., 2014). The basic idea in CSP is to optimize the spatial filters such that the variance of the projected signal is maximum for one class and minimum for another class (Blankertz et al., 2008; Ge et al., 2014; Ramoser et al., 2000). CSP is originally proposed for binary classification, which has been extended to multi-classes by pairing any two classes (Dornhege et al., 2006; Ge et al., 2014) or considering any one-vs-the-rest classes (Blankertz et al., 2003; Ge et al., 2014). This is a supervised method and mostly suitable for the two-class classification problem. Despite its most popular use in the EEG classification, CSP-based features have shown some vulnerability in the presence of noise, artifacts, and nonstationarity, which are normally present in the EEG recordings. Hence, a lot of algorithms were

subsequently proposed to address this problem by employing a regularization strategy to reduce the variability of the features between training and testing sessions (Quionero-Candela et al., 2009; Sugiyama et al., 2007) and to transfer the changes between subjects performing the same experiments (Kang et al., 2009; Lotte and Guan, 2010, 2011; Samek et al., 2013b). To address the robustness issue, a recent approach formulated the problem as extracting the spatial filter computation as a divergence maximization problem (Samek et al., 2013a,b,c, 2014). This formulation integrated many state-of-the-art CSP variants and provides an information geometric interpretation.

Different from the CSP-based FE method, in which the label information of the training data is needed to guide the FE process, the complex wavelet transform (DTCWT)-based approach is an unsupervised FE method (Yang et al., 2012, 2013a,b, 2014). The wavelets were designed such that the two wavelets of the first pair were offset from one another, and another pair formed an approximate Hilbert transform pair (Yang et al., 2014). The selection of the DTCWT not only lies in the general advantages of wavelet transform, eg, EEG data at different frequency bands as well as time localization can be obtained, but also lies in the special properties that DTCWT possesses, ie, shift-invariant, approximately analytic for real and imagery parts of the filters and antialiasing effects (Yang et al., 2014). In the experiments, the EEG signal sampled at 250 Hz was decomposed into five levels; in this way, the EEG data at level 5, 4, and 3, and level 2 and 1 would represent the theta, alpha, beta, and gamma rhythms, respectively. The final features for the detection of ERD/ERS were formulated by the powers and phases at different levels and directions, coarse representation of the EEG signals, and higher order statistics such as skewness and kurtosis of the powers and phases.

3.2.2 Model adaptation

How to improve the detection accuracies of MI-SW based on MI-SW model as well as MI-TM model built using data recorded from earlier sessions were investigated (Yang et al., 2013a,b, 2014). The nonstationarity of the EEG signal leads to different distributions of the features for the training and testing data (Krusienski et al., 2011; Lotte and Guan, 2011; Lotte et al., 2009; Quionero-Candela et al., 2009; Samek et al., 2013a,b,c; Shenoy et al., 2006; Sugiyama et al., 2007; Yang et al., 2014). This nonstationarity was caused by the changes in electrode locations, variations in the electrodes impedance over time, and using and not using the feedback for online testing and training sessions. Existing approaches to address the unsupervised adaptation include unsupervised covariate shift minimization by estimating the shift in distribution based on a least-square fitting, adapting the parameters of the FE methods, unsupervised classifier adaptation, and debiasing the classifier output (Krusienski et al., 2011). The nonstationarity of EEG signal leads to the degradation of the classification performance, especially when the model was built using the data collected in a session which was far from the testing session in time. Two model adaptation methods were proposed to address the nonstationarity issue (Yang et al., 2013a,b, 2014).

Different from existing methods, the proposed method built many training models by randomly sampling the training set of the data, which can be obtained

during crossvalidation evaluation. Hence, no extra process is required. In the first model adaptation method (Yang et al., 2013a), the model adaptation is done based on the feature consistency and cluster impurity (MA-FCCI). A small amount of calibration-testing data collected on the same day as the testing data were employed. The features of the training data and the calibration-testing data were first clustered. The cluster impurity was then measured. The cluster with the minimum impurity was selected, and the number of features that were consistent with the cluster label was calculated for both training and calibration-testing data. Finally, the cluster with the maximum consistency was selected. The model that was built based on the selected chunk of training data was then used to classify the testing data. This method was tested on the training model obtained by MI-SW model, ie, model obtained by classifying MI-SW vs idle, and MI-TM model, ie, model obtained by classifying MI-TM vs idle (Yang et al., 2013b). Two types of features were employed in using the MI-SW model (Yang et al., 2013a), ie, Laplacian derivatives of power (LAD-P) and DTCWT wavelet (DTCWT-W) features. Based on the selected six healthy subjects, the average accuracies of 74.29% and 72.64% were achieved for the classification of MI-SW vs idle by using LAD-P and DTCWT-W features, respectively. Model adaptation using wavelet features resulted in significant increase compared with those without model adaptation. Surprisingly, classification of MI-SW vs idle with model adaptation using the MI-TM model resulted in comparable classification accuracies for the selected six subjects, ie, 71.81%, compared with that obtained using MI-SW model, ie, 72.12%. These results were better than that obtained without model adaptation, ie, 68.75% (using MI-SW model) and 69.74% (using MI-TM model) (Yang et al., 2013b).

In the second model adaptation method, the within-class and between-class distances were calculated between the training and calibration-testing features. The maximum separation hyperplane was then calculated by the difference of the within-class and between-classes distances, which was normalized by the average covariance of them. Subsequent projecting the within- and between-classes distances to this hyperplane was done. The final ratio of projected between-classes vs within-class distances was used to determine which model to be selected, ie, MA-RBWD (Yang et al., 2014). The detection of MI-SW and MI-TM showed significant higher performance compared with existing methods such as the FBCSP, CSP, and SWDCSP, with the average cross-validation accuracy across subjects as: 70.89% and 73.79% for classifying MI-SW vs idle and classifying MI-TM vs idle, respectively. The session-to-session classification results indicated that the use of model adaptation increased the classification accuracy compared with that of no model adaptation and selecting the model with the best cross-validation accuracy, especially for the MI-TM. These results confirmed the detectability of MI-SW and MI-TM, which also validated the use of MI-TM for stroke dysphagia rehabilitation.

3.3 NEURAL CORTICAL CORRELATES OF MI-SW WITH ME-SW

In the last several years, several groups have conducted experiments to examine the correlates of MI-SW and motor execution of swallow (ME-SW) based on different

modalities such as EEG (Yang et al., 2015a,b) and NIRS (Kober and Wood, 2014; Kober et al., 2015). Identifying the neural cortical correlates of MI-SW with that of ME-SW is important so as to employ MI-SW for the treatment of dysphagia patients. Comparable and overlapping activation of brain areas for MI-SW and ME-SW may help promote the use of MI-SW in developing practical rehabilitation tools for the training of stroke dysphagia patients. The first attempt was to use NIRS to study the hemodynamic changes in the brain that respond to MI-SW and ME-SW (Kober and Wood, 2014; Kober et al., 2015). NIRS is a noninvasive optical imaging technique which measures the concentration changes of oxyhemoglobin (oxy-Hb) and deoxygenated hemoglobin (deoxy-Hb) in the cerebral vessels based on the absorption spectra for light in the near-infrared range (Kober et al., 2015). oxy-Hb and deoxy-Hb are important indicators of the changes in the cerebral blood flow, which are also the indicators of cortical brain activation (Kober et al., 2015). Compared with other neuroimaging modalities such as fMRI, NIRS is cheaper, more portable, and offer better temporal resolution, thus allowing it to be used in patient's home.

Fourteen healthy subjects participated in this experiment (Kober and Wood, 2014). The subjects were asked to swallow a cup of water at room temperature or to imagine swallowing the same cup of water without actually drinking it. The action time for each task is 15 s, interspaced with a rest period of 28–32 s between any two tasks. Sixteen photodetectors and 16 light emitters were used to assess the relative concentration changes of oxy-Hb and deoxy-Hb. The false discovery rate (FDR) method was used to control the proportion of false positives among the channels that are detected as significant. Preprocessing of the NIRS signal was performed before the analysis, which includes rejecting the artifactual trials based on amplitude, and filtering the signal with 0.01 Hz high-pass filter and 0.90 Hz low-pass filter. The signal was then baseline corrected (eg, using the signal from −5 to 0 s) and averaged for each task (eg, MI-SW and ME-SW) separately for the time period after the task. Fig. 6 illustrates the topographical distribution of relative concentration changes in oxy- and deoxy-Hb for the different tasks.

Results from Fig. 6 revealed that the relative concentration changes in oxy- and deoxy-Hb were the strongest for channels 4 and 31 during ME and MI ($p >$ FDR 0.05). Channels 1, 27, 8, 34, 5, 30, 11, and 38 showed the second strongest signal change. These results demonstrated that changes in oxy-Hb and deoxy-Hb during MI and ME were the most pronounced in the inferior frontal gyrus including the Broca's area. Specifically, oxy-Hb was higher during ME than during MI, and oxy-Hb was significantly higher during pause than that during ME. The oxy-Hb was significantly increased during and after ME, whereas a decrease in oxy-Hb for MI was observed due to the inhibition mechanisms of motor imagery. Furthermore, the responses of deoxy-Hb of ME and MI were similar, eg, changes in deoxy-Hb showed strong positive correlation during ME-SW and MI-SW. An illustration of the time course of oxy- and deoxy-Hb during MI and ME is shown in Fig. 7.

Another interesting finding from this work was that the same deoxy-Hb level during MI and ME was observed for the group with kinesthetic MI strategy, whereas significant higher deoxy-Hb during MI than during ME was observed for the group with no strategy. It should be noted that the sensorimotor cortex, the supplementary
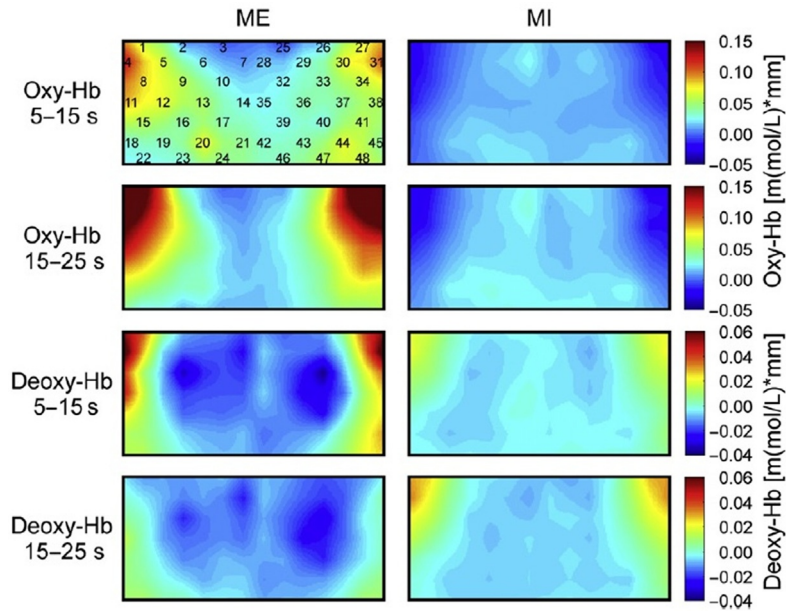
FIG. 6

Topographical distribution of relative concentration changes in oxy- and deoxy-Hb for the different tasks.

Reprinted from Kober, S.E., Wood, G., 2014. Changes in hemodynamic signals accompanying motor imagery and motor execution of swallowing: a near-infrared spectroscopy study. Neuroimage 93 (Pt. 1), 1–10, with permission from Elsevier.

FIG. 7

Mean activation changes in oxy- and deoxy-Hb in response to motor execution (ME, *black lines*) and motor imagery (MI, *gray lines*), for the left inferior frontal (LF) and right inferior frontal (RF) brain regions.

Reprinted from Kober, S.E., Wood, G., 2014. Changes in hemodynamic signals accompanying motor imagery and motor execution of swallowing: a near-infrared spectroscopy study. Neuroimage 93 (Pt. 1), 1–10, with permission from Elsevier.
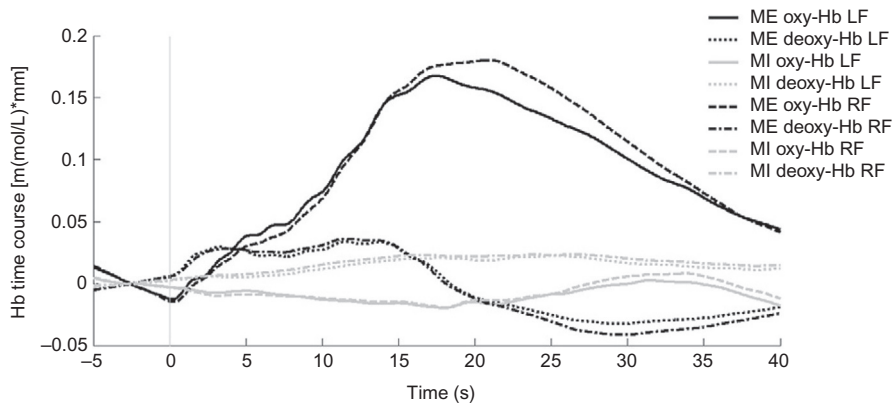
motor cortex, and anterior cingulate gyrus that were usually activated in previous imaging studies were not found in this work (Furlong et al., 2004, Martin et al., 2004). Possible reasons maybe the use of water swallowing instead of saliva swallowing that were used in earlier work, where different sensorimotor processing was employed. Distilled water may invoke gustatory sensations, reflexive swallowing such as saliva swallowing was mainly represented at the sensorimotor cortex, whereas voluntarily initiated swallowing was represented in multiple cortical regions.

Furthermore to the correlations analyzed using NIRS, the correlations between MI-SW and MI-TM, and the correlations between MI-SW and ME-SW based on 10 healthy subjects and 1 dysphagia patient were analyzed using EEG signals (Yang et al., 2015a,b). The spectral power for each trial was calculated for the EEG signal epoched at the selected time segment and electrode, and filtered at the specified frequency band. Note that the power of the baseline of 2 s was removed in calculating the spectral power. The spectral powers were averaged across trials and divided into bins for different time points, and then the accumulated spectral power at each bin, namely, the bin-based accumulated spectral powers (BASPs) was calculated. The Pearson correlation coefficients were calculated between the BASPs of MI-SW and BASPs of MI-TM, and between the BASPs of MI-SW and BASPs of ME-SW for the selected pair of channels. In the analysis, "C3" and "C4" were selected due to the reason that these regions are close to the activation regions of swallowing and tongue movements (Furlong et al., 2004, Martin et al., 2004). Significant ERD was observed at the primary motor cortex and primary somatosensory motor cortex (eg, broadmann areas 4 and 2) for water infusion and tongue thrust (Furlong et al., 2004). Furthermore, the overlapping activation for swallow and tongue movements was observed in the SMA (Martin et al., 2004). The group analysis results of using bin-based spectral powers demonstrated that MI-SW and MI-TM, and MI-SW and ME-SW were strongly correlated (p-value < 0.001, examined at "C3") for both mu and low beta frequency bands. The correlation was decreased for the dysphagia patient; nevertheless, it was still significant for MI-SW and ME-SW (p-value < 0.05) and MI-SW and MI-TM (p-value < 0.01). These results furthermore validate the use of MI-SW and MI-TM for dysphagia rehabilitation.

3.4 IMPLICATIONS FOR CLINICAL USE

To move the research from the laboratory to clinical trials, and home care of the dysphagia patients, one stroke dysphagia patient of 56-year-old male participated in the investigation (Yang et al., 2014). The patient has severe brain stem hemorrhagic stroke involving the right hemipons and midbrain. He has tetraparesis and severe poststroke dysphagia with complete dependence on nasogastric tube feeding. FEES showed the presence of moderate oropharyngeal dysphagia with reduced orolingual control, delayed swallows, mild reduced hyolaryngeal excursion, and pharyngeal stripping (Yang et al., 2014). Two sessions of EEG data were collected for both

MI-SW data and MI-TM data. In particular, each session consisted of 40 trials of MI-SW and 40 trials of idle, and 40 trials of MI-TM and 40 trials of idle for MI-SW data and MI-TM data, respectively. Not surprisingly, the accuracies of this patient on the classification of MI-SW vs idle for the two sessions were 54.95% and 77.86%, and the accuracies of classifying MI-TM vs idle for the two sessions were 78.28% and 62.19%. This observation furthermore validated the detectability of the MI-SW and MI-TM from baseline idling state for stroke dysphagia patient.

Another study on the hemodynamic signal changes during MI-SW and ME-SW for four stroke dysphagia patients and two healthy subjects using NIRS was conducted (Kober et al., 2015). The objective of this study was to observe the differences in cerebral activation patterns during swallowing for different lesion locations. The assumption was that lesions at the cerebral regions would impair voluntary swallowing and lesions at the brain stem would impair more voluntary phases of swallowing. In this work, two stroke patients with cerebral lesions in the right hemisphere, two stroke patients with lesions in the brain stem, and two healthy subjects with comparable age and gender to that of patients participated in the experiments. The protocol was similar to their earlier work (Kober and Wood, 2014), 20 trials which consisted of half MI and half ME were performed, each trial took 15 s, and there were 28–32 s of rest between any two trials. Eight photodetectors and eight light emitters were employed, resulting in 20 channels in total. The dysphagia patients with lesions in the brain stem showed bilateral hemodynamic signal changes in the inferior frontal gyrus during ME-SW compared with healthy subjects, whereas dysphagia patients with cerebral lesions in the right hemisphere showed stronger increase in oxy-Hb and deoxy-Hb during swallowing (Kober et al., 2015). This was in line with previous findings that the healthy hemisphere showed a lower activation as compared with the affected hemisphere. In addition, prolonged response time was required for patients with cerebral lesions compared to the other two groups. In summary, the topographical distribution patterns and the time course of the hemodynamic response depend on the lesion location. The increased activation during swallowing in the inferior frontal gyrus including the Broca's area, which may be due to the activation in the insula lying in the proximal area deeper inside the brain structures. Insula has been reported to be involved in the swallowing process in many earlier studies (Hamdy et al., 1999a,b, Martin et al., 2001). Overall, MI-SW and ME-SW led to comparable brain activation patterns in stroke patients, especially for the deoxy-Hb, which was consistent with the findings for young healthy subjects (Kober and Wood, 2014). The relative concentration change of oxy-Hb is stronger for ME compared with that of MI.

The limitation of the research to date is the small sample sizes for stroke dysphagia patients. In order to bring the technology from laboratory to home care, a large population of patients with various loci of lesion should be recruited in the future clinical trials. This not only to validate the hypothesis of detectability of MI-SW and MI-TM from baseline idling state but also to validate the difference in topographical distribution patterns and the time course of the hemodynamic response for stroke patients with different lesion locations.

4 DETECTION OF MI-TM

It is noticeable that there is little research work that is dedicated for detection of MI-TM for rehabilitation. Most research employed the competition data, eg, BCI competition IV dataset 2a (Ang et al., 2012; Coyle et al., 2010; Naeem et al., 2006; Tangermann et al., 2012). Dataset 2a comprised 22 channels of 9 subjects performing 4 classes of motor imagery of left hand (MI-LH), motor imagery of right hand (MI-RH), motor imagery of feet movement (MI-FM) and MI-TM (Ang et al., 2012; Coyle et al., 2010; Ge et al., 2014; Morash et al., 2008; Naeem et al., 2006). The use of independent components analysis (ICA) for the classification of multiclass of motor imagery of EEG signals was investigated (Naeem et al., 2006); however, the performance was not good compared with that of CSP. The investigation on the use of time segment before movements or imagery execution to predict the task could be useful to shorten the waiting time especially for an online training scenario (Morash et al., 2008). The combination of neural time-series prediction preprocessing (NTSPP), along with spectral filtering (SF) and CSP can significantly improve the classification performance (Coyle et al., 2010). Furthermore, none of these approaches have compared the detectability of MI-SW and MI-TM, not to mention their use for the rehabilitation of dysphagia patients. A summary of the methods for the detection of multiclass motor imagery of EEG signals including MI-TM is presented in Table 3 and discussed in detail later. It is worth noting that the focus of this section is to review existing methods that performed classification or detection of motor imagery of tongue signals in a two-class or multiclass settings; hence, it may not cover all relevant methods for a particular technique.

4.1 ICA AND FBCSP-BASED DETECTION

Different ICA methods were studied on the classification of four-classes motor imagery of EEG signals for BCI competition IV dataset 2a (Naeem et al., 2006). Three ICA methods were investigated: Infomax, FastICA, and second-order blind identification (SOBI). Infomax tries to minimize the mutual information among the extracted components, FastICA separately maximizes the negentropy of each mixture, and SOBI relies on the stationary second-order statistics that are obtained by joint diagonalization of covariance matrices (Naeem et al., 2006). CSP computes the spatial filters such that the variances of the band-pass filtered time series are maximized and optimally discriminable with respect to the different motor imagery classes. To apply CSP for the classification of multiple classes, multiple one-vs-rest filters are to be computed. Selection of the important components in ICA was done by visual inspection based on the priori knowledge of the physiological processes underlying the motor imagery (Naeem et al., 2006). Such priori knowledge can be the contralateral regions over motor cortex containing mu or beta rhythms for hand motor imagery, the midcentral or parietal components containing localized and prominent activity for foot or tongue imagery. Once the important components were selected, the logarithmic band power features for the frequency bands of alpha

Table 3 Detection of Motor Imagery of Tongue (in Multiclass Settings)

Study, Type	# of Subjects, Trials, Classes, Cue, Modality	Features, Classifiers	Accuracy/Statistical Analysis Result	Key Findings
Naeem et al. (2006) ICA	8 Healthy subj.; cue: arrow, EEG, BCI Comp. IV2a, 288 trials, 2 sess., 4 classes	All and selected components, band power features ICA (Infomax, FastICA, and SOBI)	*CV (s1/s2)*: 59.8%/63.3% (Info) 70%/73.7% (fast), 56.1%/67.6% (SOBI), 69.2%/67.0% (CSP). *S2S (s1/s2)*: 59.7%/66.7% (Info), 61.5%/65.6% (fast), 55.6%/51.7% (SOBI), 60.0%/63.6% (CSP)	○ Infomax performed better than FastICA and SOBI, but still lower than CSP ○ SOBI has fewer parameters to tune
Ang et al. (2012) FBCSP	9 Healthy subj.; cue: arrow, EEG, BCI Comp. IV2a (288 trials, 2 sess., 4 classes) & 2b (train: 240 trials/no feedback; 160 trials/feedback, eval.: 320 trials, 2 sess.)	FBCSP features, feature selection, multiclass FBCSP	*Avg. Kappa*: CV DS2a: 0.613 (DC), 0.658 (PW), and 0.663 (OVR); CV DS2b: 0.493 (MIBIF), 0.502 (MIRSR); S2S DS2a: 0.52 (DC), 0.57 (PW), and 0.57 (OVR); S2S DS2b: 0.59 (MIBIF), 0.60 (MIRSR)	○ Automatic feature selection of subject-specific frequency bands based on MIBIF and MIRSR yielded better results ○ Extending to multiclass classification of FBCSP still yielded good results
Morash et al. (2008) Pred.-BCI	8 Healthy subj. (5/3: male/female); cue: arrow & diamond; EEG for MI/ME of LH-SZ, RH-SZ, Ton-P, RF-TC, 29 electrodes at central and parietal areas; 300 trials (ME), 300 trials (MI), 4 classes	*CNV visu.*: low-pass filt., avg. volt. *ERS/ERD visu.*: power spectra *Classification*: ICA & DWT filt., norm., FS: Bayesian CV and Bhat. dist. NBC classifier	*4-class ME/MI, Avg. Acc.*: ME: 40.88% MI: 37.63% *2-class ME/MI, Avg. Acc.*: ME: 63.33%, best pair-RL: 66% MI: 60.5%, best pair-RF: 63%	○ Independence between CNV and ERD/ERS. Best pairs for classification were not consistent ○ Preparation ERD/ERS correlated better with MI prediction accuracy than ME ○ For best subject, right foot and left hand signals were the easiest to differentiate, difficult to differentiate tongue movements and other preparations

Coyle et al. (2010) PSSP-MBCI	9 Healthy subj. for BCI IV 2a (288 trials, 2 sess., 4 class), 22 electrodes; 5 healthy subj. for BCI IIIa (360 trials-first subj.; 240 trials-next 4 subj., 4 classes), 22 electrodes were chosen	NTSPP-SF, SF-CSP, NTSPP-SF-CSP LDA classifier	*5 × 5 CV*: NTSPP-SF (3 electrodes): 57.12% ± 11.66; SF-CSP (22 electrodes): 65.31% ± 14.23; NTSPP-SF-CSP (22 electrodes): 67.55% ± 11.79; *Train-Test*: NTSPP-SF (3): 54.85% ± 11.17; SF-CSP (22): 63.80% ± 14.15; NTSPP-SF-CSP (22): 67.01% ± 13.79	○ Extend the work that combines prediction based on NTSPP along with SF and CSP for 4-class MI-BCI ○ NTSPP and CSP can be combined as complementary approaches ○ NTSPP can minimize the number of channels required ○ Computation time should be minimized when NTSPP is deployed
Ge et al. (2014) STFT	3 Healthy subj. Cue: arrow, EEG, single channel, total used 6 channels; BCI Comp. IIIa, 360 trials for first subj., 240 trials second & third subj., 4 classes	Short-time fourier transform-based CSP features	*STFT + CSP*: 73.4%, 78.3%, and 75.2% (FP2, for subj. K3, K6, L1); 71.3%, 88.1%, and 71.2% (C4, for subj. K3, K6, L1)	○ No significant differences in accuracies using C3, Cz, and C4, compared with Fp1, Fpz, and Fp2 ○ Using STFT to transform time domain signal of a single channel to multiple frequency-domain signals is effective

Sess., *session;* subj., *subject;* eval., *evaluation;* visu., *visualization;* avg., *average;* volt., *voltage;* DS, *dataset;* Bhat., *Bhattacharyya;* filt., *filtered/filtering;* norm., *normalization;* FS, *feature selection;* NBC, *naive Bayesian classifier;* hemi., *hemisphere;* comp., *competition;* pred., *prediction;* DC, *divide-and-conquer;* PW, *pair-wise;* OVR, *one-vs-rest;* MIBIF, *mutual information-based best individual feature selection;* MIRSR, *mutual information-based rough set reduction.*

(eg, 10–12 Hz) and beta (eg, 16–24 Hz) rhythms were computed, forming 12 band power features for 6 components (Naeem et al., 2006). Comparison of the performance for different ICA algorithms showed that Infomax performed best by using all 22 components and the 6 selected components, but the performance was still not better than that of CSP. This better performance of CSP may be due to its supervisory nature. SOBI's overall performance was poor, which was even worse than that of Laplacian or bipolar derivations, indicating that the time delay model may not be suitable to represent ERD/RES-related brain dynamics. Robustness was also an issue for Infomax and FastICA which might be due to the optimization process, eg, the global minimum was sensitive to the choice of the initial values. On the other hand, SOBI was fast with the least number of tunable parameters that need to be adjusted. Laplacian derivations performed comparably to that of Infomax and better than that of FastICA and SOBI. Future research using automatic component selection based on a carefully designed objective measure may improve ICA-based methods. The low performance of this method may hinder its deployment for practical rehabilitation systems.

The FBCSP was proposed to optimize the subject-specific frequency band for CSP based on dataset 2a and 2b of BCI competition IV (Ang et al., 2012). Noted that dataset 2b consisted of 3 bipolar EEG channels for 9 subjects performing MI-LH and MI-RH. Extending FBCSP for the classification of multiclasses EEG signals was made by divide-and-conquer (DC), pair-wise (PW), and one-vs-rest (OVR) approaches. Two methods were proposed to select the subject-specific frequency bands by mutual information-based best individual feature (MIBIF) selection, and the mutual information-based rough set reduction (MIRSR). The experimental evaluation showed that FBCSP yielded the best performance among all the submitted algorithms for both cross-validation and session-to-session transfer.

4.2 PREDICTIVE-SPECTRAL-SPATIAL PREPROCESSING FOR A MULTICLASS BCI, PREDICTION BCI, AND SHORT-TIME FOURIER TRANSFORM-BASED DETECTION

Combination NTSPP, along with SF and CSP for multiclass BCI, namely, predictive-spectral-spatial preprocessing for a multiclass BCI (PSSP-MBCI), was investigated (Coyle et al., 2010). NTSPP exploited the differences in prediction outputs produced by different prediction networks to help improve the separability of the EEG data. The self-organizing fuzzy network was employed for prediction. The EEG signal was preprocessed with NTSPP and spectrally filtered in the subject-specific frequency bands, eg, the frequency which covers mu and beta bands were employed to detect the ERD and ERS during MI. Finally, CSP was applied to reduce the dimensionality of the data as well as to extract the effective features. The results showed that NTSPP combined with SF and CSP yielded significantly better performance than that obtained by NTSPP for the montages with 2 and 3 channels. Furthermore, NTSPP-SF without CSP also yielded better results than SF-CSP, which implied that NTSPP could be an alternative to CSP for preprocessing.

The viability of a movement/imagery prediction BCI to discover the best EEG signals for controlling a device was investigated (Morash et al., 2008). A prediction BCI was proposed that used the brain signals preceding movements execution and imagery to predict which of the four movements, ie, left hand squeeze (LH-SZ), right hand squeeze (RH-SZ), tongue press (Ton-P), and right foot toe curl (RF-TC) would occur. This prediction could potentially reduce the waiting time between a patient's action and BCI's response. Two stimulus were employed (S1 and S2), where the instruction was given at S1 to instruct the subject which action to perform. The contingent negative variation (CNV) and the ERD/ERS were unique to movement and imagery preparation. Their assumption was that the ERD/ERS would work better than that of CNV due to its straightforward relationship with motor cortex activities (Morash et al., 2008). CNV visualizations were created by low-pass filtering and averaging voltages. ERD/ERS visualizations were created by computing power spectra for each trial with hanning window and averaged at 3.9 Hz, 256 ms bins of power spectra. The data were filtered using ICA and DWT and then normalized to zero mean and unit variance. Bayesian crossvalidation and Bhattacharyya distances were employed to identify the best features for classification of movements/imagery preparations during 1.5 s before action appearance. A naive Bayesian classifier was employed as the classifier. Results showed that the CNVs and ERD/ERS were independent from each other. Each subject had particular pairs of movement/imagery that produced better results, which were not consistent among the subjects. Furthermore, less M1 activity was involved in motor imagery preparation compared with that of motor movements. The preparatory ERD/ERS correlated better with the accuracy of MI than that of ME. It was expected that the BCI would perform best when using ERD/ERS ME/MI from M1. Furthermore, they expected that classification of RH-SZ and RF-TC pair should perform better since their representations were in left and right hemispheres, respectively. However, the results showed that the best pair was the classification of LH-SZ and RF-TC pair.

How to extract the effective features of motor imagery from a system comprising only a few channels is an interesting problem. The short-time Fourier transform (STFT) was employed for the detection of motor imagery of EEG signals from few channels or a single channel (Ge et al., 2014). CSP would fail if the EEG signal only has one single channel even if it can be applied to the signal with small number of channels. The authors proposed to treat the multiple frequency bands (8–30 Hz) as a variable, thus obtained the multifrequency time varying inputs, for which the CSP can be applied. BCI competition dataset IIIa which consisted of three subjects performing MI-LH, MI-RH, MI-FM, and MI-TM was employed for evaluation. In this study, channels of C3, Cz, C4, FP1, FPz, and FP2 were selected. Experimental evaluation showed that there were no significant difference in the accuracies obtained by using channels located at the motor cortex (eg, C3, Cz, and C4) compared with those obtained using channels located far from the motor cortex (eg, FP1, FPz, and FP2). This finding coincides with the findings that high correlations in the event-related potential and spectral perturbation were found at the forehead area and sensorimotor area EEGs during a motor imagery task (Li et al., 2009). Furthermore,

employing STFT to transform the time domain signal of a single channel into multiple frequency-domain signals is effective for the detection of motor imagery EEG signals.

Other approaches that employed STFT to extract features for EEG signals of MI-LH and MI-RH were investigated (Coyle et al., 2005). Features were extracted by interpolating the spectrum obtained by calculating the norm of power in the subject-specific frequency bands. Two windows, ie, the FE window and STFT window, were employed. The temporal resolution was achieved within each FE window by sliding the STFT window along the data sequence with certain overlapping. Parameters that had a significant effect on the performance were to be tuned, which were width of the frequency bands, window length of the FE window and STFT window, overlapping between STFT windows and interpolation interval. Comparable performance was achieved by tuning the parameters compared with other existing approaches. How to develop a fully automated procedure to select the subject-specific frequency bands as well as to optimize the subject-specific parameters is an interesting research direction.

5 IMPLICATIONS AND FUTURE DIRECTIONS
5.1 FUTURE DIRECTIONS FOR NEURAL ANALYSIS OF SWALLOWING

Future studies can look at the functional interactions between the cortical swallowing regions and their relation with the brain stem central pattern generator (Hamdy et al., 1996). The poor temporal resolution and good spatial resolution of fMRI, and the poor spatial resolution and good temporal resolution of EEG, may suggest the use of a multimodal approach for the detection and analysis of the swallowing and MI-SW for stroke rehabilitation. The strong sensory input from the tongue engaged in the whole cortical swallowing network may be the primary driver of the temporal concordance between each of the cortical loci for sensory preswallow and sensory motor swallow phases (Furlong et al., 2004). The importance of the sensory input may imply that future treatments of swallowing problems after stroke might be more effective if sensory stimulation techniques are used (Furlong et al., 2004). For example, some forms of oral/tongue stimulation may help accelerate the swallowing recovery. The difference in the activation for mild and severe dysphagic patients and controls can also be due to their behavioral differences (Teismann et al., 2011). As a result, a parametric scanning design can be designed with different levels of swallowing tasks. No significant difference in BP and PMP amplitude between volitional swallowing and tongue protrusion was found (Satow et al., 2004), which may imply that the SMA may not play any specific role in volitional swallowing. Hence, future work on functional significance of SMA in swallowing on larger number of patients is needed. Current work has investigated the neural correlates MI-SW and ME-SW based on NIRS; future work can concentrate on investigating the neural correlates between MI-SW and MI-TM, and between MI-SW and ME-SW, which will form the neural basis in the use of BCI-based rehabilitation for dysphagia patients.

Combining sensory stimulation with BCI-based training techniques may also benefit the recovery of the dysphagia patients.

5.2 FUTURE DIRECTIONS ON THE REHABILITATION OF STROKE DYSPHAGIA PATIENTS

The main challenges in employing the motor imagery for the rehabilitation of stroke dysphagia patients lie in the followings. First, it is relatively difficult to imagine the complex swallowing process compared with that of motor imagery of upper limb and low limb. This is especially true for the dysphagia patients who might have difficulty initiating the swallow process. Hence, we suggest the rehabilitation should be targeting at those patients with mild dysphagia considering the safety and efficacy of the technique. An example of the suggested rehabilitation for dysphagia patient by incorporating the motor imagery technique is shown in Fig. 8.

Two strategies for rehabilitation are suggested in this review. In the first strategy, the engagement of the patients during motor imagery process is measured by coupling the MI-SW or MI-TM with the traditional swallowing therapies, eg, using the detected MI-SW or MI-TM signal to trigger an actual swallow and provide feedback to the patient (Ang et al., 2014a,b; Prasad et al., 2010; Silvoni et al., 2011). In this way, a speech and language therapist is required to assist the patient with the actual swallowing. It is reasonable to employ MI-TM instead of MI-SW if the patient is unable to perform MI-SW or in a severe situation. A practical deployment is to perform MI-TM in the training sessions, and perform MI-SW in online rehabilitation sessions. In the second strategy, the detected MI-SW or MI-TM signal can be used as a switch or trigger for subsequent neuromuscular or oral sensory stimulation (Kiger et al., 2006; Langdon and Blacker, 2010; Silvoni et al., 2011). The stimulation
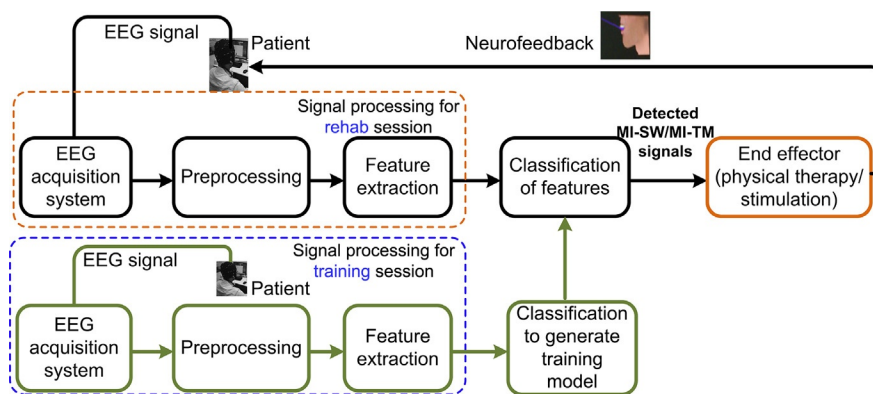

FIG. 8

Block diagram illustrating a motor imagery-based rehabilitation system for dysphagia patients.

location should be carefully selected, eg, the hyoid bone for neuromuscular stimulation. Furthermore, the strength of the stimulation should be varied according to the severeness of the patient. The patient to use the stimulation therapy should be able to establish the basic swallow pattern for the sake of safety. Consultation with the speech and language therapist and doctors is required regarding the safety on the use of stimulation technique for the patients (Langdon and Blacker, 2010).

REFERENCES

Ang, K.K., Guan, C., 2015. Brain–computer interface for neuro-rehabilitation of upper limb after stroke. Proc. IEEE 103 (6), 944–953. 06/2015.

Ang, K.K., Chin, Z.Y., Wang, C., Guan, C., Zhang, H., 2012. Filter bank common spatial pattern algorithm on BCI competition IV datasets 2a and 2b. Front. Neurosci. 6, 39.

Ang, K.K., Chua, K.S.G., Phua, K.S., Wang, C., Chin, Z.Y., Kuah, C.W.K., Low, W., Guan, C., 2014a. A randomized controlled trial of EEG-based motor imagery brain-computer interface robotic rehabilitation for stroke. Clin. EEG Neurosci. 45, 1–11.

Ang, K.K., Guan, C., Phua, K.S., Wang, C., Zhou, L., Tang, K.Y., Joseph, G.J.E., Kuah, C.W.K., Chua, K.S.G., 2014b. Brain computer interface-based robotic end effector system for wrist and hand rehabilitation: results of a three-armed randomized controlled trial for chronic stroke. Front. Neuroeng. 7, 30.

Blankertz, B., Dornhege, G., Schafer, C., Krepki, R., Kohlmorgen, J., et al., 2003. Boosting bit rates and error detection for the classification of fast-paced motor commands based on single-trial EEG analysis. IEEE Trans. Neural Syst. Rehabil. Eng. 11, 127–131.

Blankertz, B., Tomioka, R., Lemm, S., Kawanabe, M., Muller, K.-R., January 2008. Optimizing spatial filters for robust EEG single-trial analysis. IEEE Signal Process. Mag. 41, 41–56.

Coyle, D., Prasad, G., McGinnity, T.M., 2005. A time-frequency approach to feature extraction for a brain-computer interface with a comparative analysis of performance measures. EURASIP J. Adv. Signal Process. 2005 (19), 3141–3151. http://dx.doi.org/10.1155/ASP.2005.3141.

Coyle, D., Satti, A., Mcginnity, T.M., 2010. Predictive-spectral-spatial preprocessing for a multiclass brain-computer interface. In: The 2010 International Joint Conference on Neural Networks (IJCNN), pp. 1–8.

de Vries, S., Mulder, T., 2007. Motor imagery and stroke rehabilitation: a critical discussion. J. Rehabil. Med. 39, 5–13.

Dickstein, R., Deutsch, J.E., 2007. Motor imagery in physical therapist practice. Phys. Ther. 2007 (87), 942–953.

Dickstein, R., Dunsky, A., Marcovitz, E., 2004. Motor imagery for gait rehabilitation in post-stroke hemiparesis. Phys. Ther. 84, 1167–1177.

Do, A.H., Wang, P.T., King, C.E., Abiri, A., Nenadic, Z., 2011. Brain–computer interface controlled functional electrical stimulation system for ankle movement. J. Neuroeng. Rehabil. 8, 1–14.

Do, A.H., Wang, P.T., King, C.E., Chun, S.N., Nenadic, Z., 2013. Brain–computer interface controlled robotic gait orthosis. J. Neuroeng. Rehabil. 10, 111.

Dornhege, G., Blankertz, B., Krauledat, M., Losch, F., Curio, G., et al., 2006. Combined optimization of spatial and temporal filters for improving brain computer interfacing. IEEE Trans. Biomed. Eng. 53, 2274–2281.

Dunsky, A., Dickstein, R., Marcovitz, E., Levy, S., 2008. Home-based motor imagery training for gait rehabilitation of people with chronic post-stroke hemiparesis. Arch. Phys. Med. Rehabil. 89, 1580–1588.

Ertekin, C., Aydogdu, I., 2003. Neurophysiology of swallowing. Clin. Neurophysiol. 114 (12), 2226–2244.

Furlong, P.L., Hobson, A.R., Aziz, Q., Barnes, G.R., Singh, K.D., Hillebrand, A., Thompson, D.G., Hamdy, S., 2004. Dissociating the spatio-temporal characteristics of cortical neuronal activity associated with human volitional swallowing in the healthy adult brain. Neuroimage 22, 1447–1455.

Ge, S., Wang, R., Yu, D., 2014. Classification of four-class motor imagery employing single-channel electroencephalography. PLoS One 9, e98019.

Hamdy, S., Aziz, Q., Rothwell, J.C., Singh, K.D., Barlow, J., Hughes, D.G., Tallis, R.C., Thompson, D.G., 1996. The cortical topography of human swallowing musculature in health and disease. Nat. Med. 2 (11), 1217–1224.

Hamdy, S., Aziz, Q., Rothwell, J.C., Crone, R., Hughes, D., Tallis, R.C., Thompson, D.G., 1997a. Explaining oropharyngeal dysphagia after unilateral hemispheric stroke. Lancet 350, 686–692.

Hamdy, S., Aziz, Q., Rothwell, J.C., Power, M., Singh, K.D., Nicholson, D.A., et al., 1998. Recovery of swallowing after dysphagic stroke relates to functional reorganization in the intact motor cortex. Gastroenterology 115, 1104–1112.

Hamdy, S., Mikulis, D.J., Crawley, A., Xue, S., Lau, H., Henry, S., Diamant, N.E., 1999a. Cortical activation during human volitional swallowing: an event-related fMRI study. Am. J. Physiol. 277 (1 Pt. 1), G219–G225.

Hamdy, S., Rothwell, J.C., Brooks, D.J., Bailey, D., Aziz, Q., Thompson, D.G., 1999b. Identification of the cerebral loci processing human swallowing with H2(15)O PET activation. J. Neurophysiol. 81 (4), 1917–1926.

Hamdy, S., Rothwell, J.C., Aziz, Q., Thompson, D.G., 2000. Organization and reorganization of human swallowing motor cortex: implications for recovery after stroke. Clin. Sci. (Lond.) 99 (2), 151–157.

Hamdy, S., Aziz, Q., Thompson, D.G., Rothwell, J.C., 2001. Physiology and pathophysiology of the swallowing area of human motor cortex. Neural Plast. 8 (1–2), 91–97.

Jestrovic, I., Coyle, J.L., Sejdic, E., 2015. Decoding human swallowing via electroencephalography: a state-of-the-art review. J. Neural Eng. 12, 051001. 15 pp.

Kang, H., Nam, Y., Choi, S., 2009. Composite common spatial pattern for subject-to-subject transfer. IEEE Signal Process. Lett. 16 (8), 683–686.

Kiger, M., Brown, C.S., Watkins, L., 2006. Dysphagia management: an analysis of patient outcomes Using VitalStim™ therapy compared to traditional swallow therapy. Dysphagia 21, 243–253.

Kober, S.E., Wood, G., 2014. Changes in hemodynamic signals accompanying motor imagery and motor execution of swallowing: a near-infrared spectroscopy study. Neuroimage 93 (Pt. 1), 1–10.

Kober, S.E., Bauernfeind, G., Woller, C., Sampl, M., Grieshofer, P., Neuper, C., Wood, G., 2015. Hemodynamic signal changes accompanying execution and imagery of swallowing in patients with dysphagia: a multiple single-case near-Infrared spectroscopy study. Front. Neurol. 6, 151.

Krusienski, D.J., Grosse-Wentrup, M., Galán, F., Coyle, D., Miller, K.J., Forney, E., Anderson, C.W., 2011. Critical issues in state-of-the-art brain-computer interface signal processing. J. Neural Eng. 8 (2), 025002. http://dx.doi.org/10.1088/1741-2560/8/2/025002.

Langdon, C., Blacker, D., 2010. Dysphagia in stroke: a new solution. Stroke Res. Treat. 2010. http://dx.doi.org/10.4061/2010/570403. 570403, 6 pages. Published online 2010 Jun 30, PMCID, PMC2915662.

Li, K.D., Sun, G.F., Zhang, B.F., Wu, S.C., Wu, G.F., 2009. Correlation between forehead EEG and sensorimotor area EEG in motor imagery task. In: Eighth IEEE International Conference on Dependable, Autonomic and Secure Computing, IEE DASC'09, pp. 430–435.

Lotte, F., Guan, C., 2010. Learning from other subjects helps reducing brain-computer interface calibration time. In: IEEE International Conference on Acoustics, Speech, and Signal Processing (ICASSP), pp. 614–617.

Lotte, F., Guan, C., 2011. Regularizing common spatial patterns to improve BCI designs: unified theory and new algorithms. IEEE Trans. Biomed. Eng. 58 (2), 355–362.

Lotte, F., Guan, C., Ang, K.K., 2009. Comparison of designs towards a subject-independent brain-computer interface based on motor imagery. IEEE EMBC 2009, 4543–4546.

Martin, R.E., Goodyear, B.G., Gati, J.S., Menon, R.S., 2001. Cerebral cortical representation of automatic and volitional swallowing in humans. J. Neurophysiol. 85 (2), 938–950.

Martin, R.E., MacIntosh, B.J., Thomas, C., Gati, J.S., Menon, R.S., 2002. Comparison of brain activation during swallowing and tongue movement: event-related fMRI. Soc. Neurosci. Abstr. 163 (12), 2002.

Martin, R.E., MacIntosh, B.J., Smith, R.C., Barr, A.M., Stevens, T.K., Gati, J.S., Menon, R.S., 2004. Cerebral areas processing swallowing and tongue movement are overlapping but distinct: a functional magnetic resonance imaging study. J. Neurophysiol. 92, 2428–2443.

Matsuo, K., Palmer, J.B., 2008. Anatomy and physiology of feeding and swallowing: normal and abnormal. Phys. Med. Rehabil. Clin. N. Am. 19 (4), 691–707.

McKeown, M.J., Torpey, D.C., Gehm, W.C., 2002. Non-invasive monitoring of functionally distinct muscle activations during swallowing. Clin. Neurophysiol. 113, 354–366.

Morash, V., Bai, O., Furlani, S., Lin, P., Hallett, M., 2008. Classifying EEG signals preceding right hand, left hand, tongue, and right foot movements and motor imageries. Clin. Neurophysiol. 119, 2570–2578.

Mosier, K., Patel, R., Liu, W., Kalnin, A., Maldjian, J., Baredes, S., 1999. Cortical representation of swallowing in normal adults: functional implications. Laryngoscope 109, 1417–1423.

Naeem, M., Brunner, C., Leeb, R., Graimann, B., Pfurtscheller, G., 2006. Seperability of four-class motor imagery data using independent components analysis. J. Neural Eng. 3, 208.

Prasad, G., Herman, P., Coyle, D., McDonough, S., Crosbie, J., 2010. Applying a brain-computer interface to support motor imagery practice in people with stroke for upper limb recovery: a feasibility study. J. Neuroeng. Rehabil. 7 (1), 60. http://dx.doi.org/10.1186/1743-0003-7-60.

Quionero-Candela, J., Sugiyama, M., Schwaighofer, A., Lawrence, N.D. (Eds.), 2009. Dataset Shift in Machine Learning. MIT Press, Cambridge, MA.

Ramoser, H., Muller-Gerking, J., Pfurtscheller, G., 2000. Optimal spatial filtering of single trial EEG during imagined hand movement. IEEE Trans. Rehabil. Eng. 8 (4), 441–446.

Samek, W., Blythe, D., Müller, K.-R., Kawanabe, M., 2013a. Robust spatial filtering with beta divergence. In: Advances in Neural Information Processing Systems 26 (NIPS), pp. 1007–1015.

Samek, W., Binder, A., Muller, K.-R., 2013b. Multiple kernel learning for brain-computer interfacing. In: International Conference of the IEEE Engineering in Medicine and Biology Society (EMBC), pp. 7048–7051.

Samek, W., Meinecke, F., Muller, K.-R., 2013c. Transferring subspaces between subjects in brain-computer interfacing. IEEE Trans. Biomed. Eng. 60 (8), 2289–2298.

Samek, W., Kawanabe, M., Muller, K.-R., 2014. Divergence-based framework for common spatial patterns algorithms. IEEE Rev. Biomed. Eng. 7, 50–72.

Satow, T., Ikeda, A., Yamamoto, J., Begum, T., Thuy, D.H., Matsuhashi, M., Mima, T., Nagamine, T., Baba, K., Mihara, T., Inoue, Y., Miyamoto, S., Hashimoto, N., Shibasaki, H., 2004. Role of primary sensorimotor cortex and supplementary motor area in volitional swallowing: a movement-related cortical potential study. Am. J. Physiol. Gastrointest. Liver Physiol. 287 (2), G459–G470.

Sharma, N., Pomeroy, V.M., Baron, J.-C., 2006. Motor imagery: a backdoor to the motor system after stroke? Stroke 37 (7), 1941–1952.

Shenoy, P., Krauledat, M., Blankertz, B., Rao, R.P., Muler, K.R., 2006. Towards adaptive classification for BCI. J. Neural Eng. 3 (1), R13–R23.

Silvoni, S., Ramos-Murguialday, A., Cavinato, M., Volpato, C., Cisotto, G., Turolla, A., Piccione, F., Birbaumer, N., 2011. Brain-computer interface in stroke: a review of progress. Clin. EEG Neurosci. 42 (4), 245–252. http://dx.doi.org/10.1177/155005941104200410.

Sugiyama, M., Krauledat, M., Muller, K.-R., 2007. Covariate shift adaptation by importance weighted cross validation. J. Mach. Learn. Res. 8, 985–1005.

Tangermann, M., Muller, K.R., Aertsen, A., Birbaumer, N., Braun, C., Brunner, C., Leeb, R., Mehring, C., Miller, K.J., Muller-Putz, G.R., Nolte, G., Pfurtscheller, G., Preissl, H., Schalk, G., Schlogl, A., Vidaurre, C., Waldert, S., Blankertz, B., 2012. Review of the BCI competition IV. Front. Neurosci. 6, 55.

Teismann, I.K., Warnecke, T., Suntrup, S., Steinstrater, O., Kronenberg, L., Ringelstein, E.B., Dengler, R., Petri, S., Pantev, C., Dziewas, R., 2011. Cortical processing of swallowing in ALS patients with progressive dysphagia—a magnetoencephalographic study. PLoS One 6 (5), e19987.

Wolpaw, J.R., Birbaumer, N., McFarland, D.J., Pfurtscheller, G., Vaughan, T.M., 2002. Brain-computer interfaces for communication and control. Clin. Neurophysiol. 113 (6), 767–791.

Yang, H., Guan, C., Ang, K.K., Wang, C., Phua, K.S., Yu, J., 2012. Dynamic initiation and dual-tree complex wavelet feature-based classification of motor imagery of swallow EEG signals. In: The 2012 International Joint Conference on Neural Networks (IJCNN), pp. 1–6.

Yang, H., Guan, C., Ang, K.K., Wang, C., Phua, K.S., Tang, C.K.Y., Zhou, L., 2013a. Feature consistency-based model adaptation in session-to-session classification: a study using motor imagery of swallow EEG signals. In: The 35th Annual International Conference of the IEEE Engineering in Medicine and Biology Society (EMBC), pp. 429–432.

Yang, H., Guan, C., Ang, K.K., Wang, C., 2013b. Detection of motor imagery of swallow with model adaptation: swallow or tongue. In: Abstract in Fifth International Brain Computer Interface Meeting 56.

Yang, H., Guan, C., Chua, K.S.G., Wang, C., Phua, K.S., Tang, C.K.Y., Ang, K.K., 2014. Detection of motor imagery of swallow EEG signals based on the dual-tree complex wavelet transform and adaptive model selection. J. Neural Eng. 11 (3), 035016.

Yang, H., Guan, C., Wang, C., Ang, K.K., Phua, K.S., Chok, S.S., Tang, C.K.Y., Chua, K.S.G., 2015a. On the correlations of motor imagery of swallow with motor imagery of tongue movements and actual swallow. In: Proceedings of the fifth International Conference on Cognitive Neurodynamics. Advances in Cognitive Neurodynamics, vol. V, pp. 397–404. Chapter 55, June 3–7, China, 2015.

Yang, H., Guan, C., Wang, C., Ang, K.K., 2015b. Detection of motor imagery of brisk walking from electroencephalogram. J. Neurosci. Methods 244, 33–44.